PHYLOGEOGRAPHY OF PALEARCTIC BIRDS USING MULTILOCUS COALESCENCE ANALYSES

A DISSERTATION
SUBMITTED TO THE FACULTY OF THE GRADUATE SCHOOL
OF THE UNIVERSITY OF MINNESOTA
BY

CHIH-MING HUNG

IN PARTIAL FULFILLMENT OF THE REQUIREMENTS
FOR THE DEGREE OF
DOCTOR OF PHILOSOPHY

ADVISED BY

ROBERT MARTIN ZINK

JULY 2012

Acknowledgments

Pursuing my Ph.D. degree in the United State has dramatically changed my life. I gained more than just a degree. I learned to be a better scientist, know friends from different countries, and explored different parts of this country. Also, I gained twin boys.

I am thankful to my advisor, Bob Zink. He always provided useful advice in my research, career and life. His delightful mentoring is one of the main reasons I enjoyed the process of pursuing my Ph.D.

My committee members, Keith Baker, Ken Kozak and Susan Weller gave me timely support and advice in my research, and I thank them for this as well as having written many recommendation letters for me.

Many friends from the Department of Ecology, Evolution and Behavior, the Conservation Biology program, the University of Minnesota or outside the campus provided company, conversation and friendship, which helped free me from some of the stresses of graduate student life. The input from these friends made my life over here much more interesting.

I thank my family immensely. My wife, I-Yu Huang, has practically been a single-mom for several years and my sons only saw their father a few months per year. I thank my parents and siblings for helping to take care of my sons. Their help was essential in allowing me to finish this Ph.D.

Abstract

The phylogeography of three widespread Palearctic passerines was characterized in this dissertation based on sequence data from mitochondrial and nuclear genes, which were analyzed under a framework of the coalescent. The following questions were addressed: (1) does gene history reflect species history, (2) does natural selection on mitochondrial DNA (mtDNA) obscure phylogeographic inference, and (3) do the early stages of speciation reveal ecological niche divergence. In chapter one, phylogeographic histories based on mtDNA and 13 nuclear genes of Eurasian nuthatches (*Sitta europaea*) were compared to address an ongoing debate over the value of mtDNA in phylogeography. Both mtDNA and multilocus nuclear data recovered the same three clades. The results suggested that mtDNA is efficient in discovering phylogeographic pattern due to its fast coalescence rate. Multiple (nuclear) genes permitted quantification and estimation of error in process parameters such as effective population size, gene flow and divergence time. Neither mtDNA alone, nuclear genes alone, or both in combination resolved the phylogenetic pattern of the three groups, leading to an inference of simultaneous divergence. In chapter two, I devised novel methods based on coalescent simulations to discover whether natural selection has influenced the mitochondrial genome of two Old World flycatcher species (*Ficedula parva* and *F. albicilla*). The simulations were based on the estimated demographic history using 18 nuclear genes, which suggested that the two sister species diverged around three million years ago and that *F. albicilla*, but not *F. parva*, experienced a recent population expansion. My analyses showed that population bottlenecks alone could not fully explain the strikingly low variation in the mtDNA data for *F. albicilla*, and I concluded that the mtDNA patterns were affected by natural

selection. Thus, interpreting the phylogeographic history based solely on mtDNA can be misleading, although the nuclear loci corroborated the species limits. Chapter three involved coalescence and simulation approaches based on mtDNA and a Z-linked gene to explore the early stages of evolutionary divergence in the common rosefinch (*Carpodacus erythrinus*). The third chapter also involved an assessment of ecological niche divergence and the results showed no evidence of ecological divergence at the early stages of diversification among three rosefinch lineages. This dissertation demonstrates that the incorporation of multiple genes, coalescence theory, and analytic approaches from other fields (e.g., ecological niche modeling) can provide fresh insights into phylogeographic history of species.

Table of Contents

List of Tables

Chapter 1

Chapter 2

List of Figures

Introduction

The study of the geographic deployment of genetic variation and its causes comprises the field of phylogeography. Although phylogeography initially aimed to integrate population genetics and phylogenetics (Avise 2000), this goal has not been fully achieved until recently when genetic variation from populations were analyzed using coalescence theory (Hickerson et al. 2009). The advances in coalescence-based approaches enable phylogeographers to quantify demographic parameters, which can explicitly illuminate the processes of lineage or species evolution. Another recent trend is the use of data from multiple loci. In the past 20 years, mitochondrial DNA (mtDNA) has been the principal genetic marker for inferring phylogeographic history of animals. Lately, the authority of mtDNA in phylogeography has been questioned (Funk and Omland 2003; Ballard and Whitlock 2004; Edwards and Bensch 2009; Galtier et al. 2009). That is because some researchers believe that stochastic processes, natural selection or hybridization can preclude mtDNA, which yields in effect a single gene tree, from reflecting species history. Multiple genes are thought to be necessary to unveil the complete history of a species. This view is thought by some to be overly simplistic or misleading (Zink and Barrowclough 2008).

This dissertation demonstrates how these two new trends, (a) the applications of coalescence theory and (b) the incorporation of multilocus data, revolutionize our interpretations in phylogeography. I studied three widespread Palearctic avian species as examples, which also adds to our understanding of the taxonomy and phylogeography of birds in the largest and relatively unstudied ecozone on Earth.

Chapter one focuses on the multilocus phylogeography of Eurasian nuthatches (*Sitta europaea*). In this chapter, I compared the mtDNA-based history with that based on multiple nuclear genes and found generally consistent results between the two datasets. Several coalescence-based approaches were applied to estimate species trees and demographic history and to test alternative species tree topologies. Whereas the results showed that mtDNA was correct in suggesting three independently evolving taxa, multiple genes provided more reliable estimates of process parameters such as effective population size, gene flow and divergence time. Therefore, I suggest using both mitochondrial and nuclear genes to obtain a comprehensive view of species history.

Chapter two examines whether population bottlenecks or natural selection caused the extremely low levels of mtDNA variation observed in a priory study of two sister species of Old World flycatchers (*Ficedula parva* and *F. albicilla*). At the ND2 gene, there was no variation observed in 75 individuals of *F. albicilla* sampled across 4,500 km of their eastern Palearctic breeding range, and the question was whether this was simply the consequence of a bottleneck. I sampled up to 18 nuclear genes to test whether positive selection affected the levels and patterns of variability in their mtDNA. Levels of genetic variability in the nuclear genes of the two species were nearly identical, unlike that for mtDNA. The multilocus dataset therefore suggested departure from neutrality. In addition, the historical population size of *F. albicilla* underwent a recent large increase. In this study, I devised a neutrality test by incorporating multilocus demographic history into a neutral coalescence simulation. I also considered models of protein structure to evaluate possible traces of positive selection. The results implied that selective forces and historical demographic fluctuation probably reduce the mtDNA

variation especially for *F. albicilla*. This study also illustrates how coalescence-based approaches and multilocus data can be applied to test for natural selection and gene history.

Chapter three explores the early stage of lineage divergence in the common rosefinch (*Carpodacus erythrinus*), another widespread Palearctic passerine bird. The results of coalescence-based programs and simulations supported a history of three recently diverged lineages, none of which can be diagnosed by mtDNA or a Z-linked gene tree alone. Instead, the lineages appear to be at too early a stage of divergence to allow coalescence of gene trees from either the mtDNA or nuclear loci. This chapter also involves an assessment of niche divergence. Some studies of birds have suggested that niches do not change until long after speciation. The results were consistent with this view, as none of the lineages exhibit significant niche divergence.

Overall, this dissertation represents a new phase in phylogeography that goes beyond discovering patterns, by exploring the underlying processes in depth. To achieve this goal, incorporating coalescence theory, multiple loci and ecological niche modeling promises to contribute to the maturity of phylogeography.

Chapter 1

Multilocus coalescence analyses support a mtDNA-based phylogeographic history for a widespread Palearctic passerine bird, *Sitta europaea*

Hung, C.-M., S. V. Drovetski, and R. M. Zink. 2012. *Evolution* (in press)

Our understanding of species phylogeography in much of the Palearctic is incomplete. In addition, many existing studies based solely on mitochondrial DNA (mtDNA) can provide a biased view of phylogeographic history because of the effects of lineage sorting, natural selection or hybridization. We analyzed 13 introns to assess a mtDNA study of the Eurasian nuthatch (*Sitta europaea*) that suggested a seemingly contemporaneous origin of distinct taxa in the Caucasus, Europe, and Asia. Neutrality tests showed no evidence of selection on either the mtDNA or nuclear sequences. Most nuclear gene trees, except for Z-linked ones, did not recover the three lineages, which we attribute to recent splitting. Analyses of the 13 introns combined revealed the same three groups as did the mtDNA and suggested that nuthatches experienced a trichotomous (or two indistinguishable) split(s) 1-2 Ma ago and have remained isolated with trifling if not zero gene flow since then, and the Asian group increased in population size. This result demonstrates the usefulness of mtDNA in discovering phylogeographic patterns. The use of multiple nuclear loci facilitated detection of an introgressed individual and improved estimates of process parameters such as divergence time and population expansion. We recommend that phylogeographic studies should be based on both mtDNA and nuclear genes.

Supplementary Material

Supporting figures 1.1-1.6 and tables 1.1-1.2 are available online.

Introduction

Phylogeography involves discovering patterns of population structure and investigating the underlying evolutionary processes leading to those structures (Beheregaray 2008; Zink and Barrowclough 2008). Both goals can be achieved through adopting genetic markers with informative evolutionary rates or coalescence times (Spellman and Klicka 2006; Zink and Barrowclough 2008; Knowles 2009; Hickerson et al. 2010). In the past two decades, our knowledge of phylogeography has been obtained mainly from studies of mitochondrial DNA (mtDNA) because of its presumed neutrality, high mutation rate, small effective population size (N_e), and lack of recombination (Avise et al. 1987; Avise 2000; Hickerson et al. 2010). However, phylogeographic studies based solely on mtDNA have been criticized due to the single-locus inheritance of mtDNA (Jennings and Edwards 2005; Dolman and Moritz 2006; Edwards and Bensch 2009). One concern is that stochastic sorting of ancestral polymorphism may render the genealogical histories of individual gene trees, such as mtDNA, misleading pictures of the organismal or species tree (Maddison and Knowles 2006; Knowles and Carstens 2007). Other authors (e.g., Ballard and Whitlock 2004; Dowling et al. 2008; Galtier et al. 2009) believe that mtDNA patterns are often biased by natural selection, rendering them erroneous estimates of population history. In addition, hybridization can lead to conflicting patterns between mtDNA trees and species trees (Maddison 1997; Funk and Omland 2003). Thus, multilocus data are useful for detecting independent lineages and penetrating the noise generated from coalescent stochasticity (Brito and Edwards 2009). Furthermore, selection is not likely to bias unlinked loci in a concordant manner (Nielsen 2005), and comparison among genes facilitates the detection of introgression (Bossu and Near 2009).

The Palearctic encompasses the largest terrestrial area on Earth (Pielou 1979), although our knowledge of its biogeography is uneven (Beheregaray 2008). In particular, the western Palearctic (Europe) has been intensively studied whereas the Asian part of the Palearctic has received less attention (Pavlova et al. 2005). There are reasons to expect phylogeographic differences between eastern and western Palearctic regions (Abbott and Brochmann 2003; Hewitt 2004). For example, Europe was covered by ice while most of the Asian Palearctic was ice-free during the Last Glacial Maximum (LGM), around 20,000 years ago (Adams 2002). In addition, the Caucasus, which include a high percentage of endemic subspecies and differentiated populations (Stepanyan 2003), is believed to have become a remote forest island 430,000 years ago based on paleontological and paleoclimatic evidence (see Tyrberg 1998; EPICA 2004). Several published mtDNA phylogeographic studies of widespread species do not support a common pattern across the Palearctic, suggesting idiosyncratic evolutionary histories (e.g., Drovetski et al. 2004; Hewitt 2004; Zink 2005; Zink et al. 2006, 2008; Haring et al. 2007; Fedorov et al. 2008). However, it is possible that the inconsistent patterns of mtDNA differentiation among species simply reflect variance in the coalescence process or the effects of natural selection – that is, biases that can affect any single locus. Thus, before we can understand the comparative phylogeographic history of species in the Palearctic, it is necessary to examine multilocus patterns in individual species to test mtDNA patterns.

The Eurasian nuthatch (*Sitta europaea*) is a widespread, sedentary Palearctic passerine. It is an obligate forest species and therefore provides an example of how the Palearctic forest fauna responded to historical climate changes. A mtDNA-based study

revealed three distinct haplogroups generally corresponding to the Asia (although Finland and Vyatka are located in Europe, we grouped them with the Asian group for convenience), Europe and Caucasus (Fig. 1.1; Zink et al. 2006). However, the evolutionary relationships among these three phylogroups were unresolved and appeared to be a trichotomy. Zink et al. (2006) detected selection against slightly deleterious alleles in the ND2 sequences of nuthatches but argued that its effect on phylogeographic inference was negligible. In this study, we (1) test whether selection acts on mtDNA or nuclear loci and obscures historical inference, (2) examine whether nuclear genes recover the three mtDNA phylogroups and whether multilocus species trees clarify their relationship, and (3) compare multilocus estimates of gene flow and population history with those from mtDNA.

Methods and Materials

Sampling and Haplotype Determination

We used ND2 sequence data (1041 bp) for 134 Eurasian nuthatches from Zink et al.'s (2006) study (NCBI accession numbers DQ219639-DQ219772) and added two samples from Germany and one sample from the Czech Republic. We sequenced 11 autosomal and two Z-linked introns for both strands in each nuthatch sample (Table 1.1) using published primers (Backström et al. 2006, 2008; Kimball et al. 2009). The ND2 sequence of a nuthatch from Markovo identified as *S. e. arctica* differs by 10% uncorrected distance from other samples (Zink et al. 2006), and this sample was used as an outgroup for phylogenetic analyses. Indels (insertions or deletions) were common among the introns, which were useful for reconstructing (phasing) haplotypes of

individuals with multiple heterozygous sites. Phases of sequences containing indels were sorted manually by subtracting chromatogram peaks upstream of the indel in the reverse primer sequences from the double peaks downstream of the indel in the forward primer sequences. This was repeated in the alternative direction and allowed the two haplotypes of a heterozygous individual to be determined (Sousa-Santos et al. 2005; Dolman and Moritz 2006; Drovetski et al. 2010). The lengths of indels can also be determined by this approach. This approach was not applied to individuals containing more than two indels due to their complex chromatograms (which were rare and excluded from further analysis). Multi-base indels were collapsed to single-base polymorphisms for further analyses.

Haplotypes of individuals with multiple heterozygous sites (in which double peaks were found in the chromatograms of both strands and the smaller peak was $\geq$ 33% of the larger one) were resolved using the software PHASE 2.1.1 (Stephens et al. 2001; Stephens and Scheet 2005). Homozygous genotypes and genotypes with single heterozygous site or with indels were set as known alleles to improve the performance of PHASE analyses. The phases of some sites could not be estimated confidently at 90% posterior probability. The phases of these ambiguous sites were resolved using Clark's (1990) parsimony algorithm to minimize the total number of haplotypes and singletons in the samples.

Intra-locus recombination rates were estimated using a Bayesian method (Li and Stephens 2003) implemented in PHASE 2.1.1. The haplotypes resolved using PHASE plus Clark's (1990) algorithm were used as input for the recombination estimation. The background recombination rate and the recombination rates between two polymorphic

sites were estimated and portrayed as 5,000 sampled points from the posterior distribution. The factors by which the estimated recombination rates exceed the background rate were calculated, and the upper and lower bounds of 95% credible interval (CI) of these values were recorded. If one or more estimated values were significantly larger than one, it means there has been significant recombination occurring between the corresponding sites. Otherwise, we assumed that there was no intra-locus recombination within the locus.

We used DnaSP 5 (Librado and Rozas 2009) to compute nucleotide diversity (π; Nei 1987) for each gene and θ (= $4N_e\mu$; Nei 1987, equation 10.3) for each gene and each haplogroup.

Neutrality Test

Hudson-Kreitman-Aguade (HKA) tests (Hudson et al. 1987) implemented in the HKA program (http://genfaculty.rutgers.edu/hey/software) were used to test the neutrality of the mtDNA and nuclear introns. The HKA test examines whether the association between the level of intra-specific (or intra-taxon) polymorphism and inter-specific (or inter-taxon) divergence departs from the expectation of an evolutionary neutral model for two or more genes. This test can distinguish between the effects of demographic history and natural selection (Ballard and Whitlock 2004). Only loci containing 5 or more individuals (10 or more nuclear sequences) for each phylogroup were included in the tests to avoid bias caused by low sample sizes. These tests were applied to the pairwise comparisons among the three haplogroups (Caucasus, Europe, and Asia) as well as to the comparison between the three haplogroups combined and a single sequence from the *S. e. arctica* sample.

Gene Trees

NETWORK 4.5.1.6 (fluxus-engineering.com) was used to generate a minimum spanning network of haplotypes (Polzin and Daneschmand 2003) for each gene. The networks might not reveal genealogical processes, but they provide a useful illustration of the clustering of alleles. The program MrBayes 3.1.2 (Ronquist and Huelsenbeck 2003) was used to reconstruct a Bayesian phylogeny for each gene based on the substitution model selected using AIC tests in Modeltest 3.7 (Posada and Crandall 1998). The majority-rule consensus tree was assembled based on two independent runs using the following conditions: 40 million steps, four chains, genealogies sampled every 1000 steps, the first 25% of the steps discarded as burn-in. Convergence was assessed using burn-in plots of likelihood values and convergence diagnostic parameters and comparing results from two independent runs.

Group Delimitation Using Multiple Nuclear Genes

We used two methods to test whether the nuclear genes combined could recover a significant pattern of population structure. First, the program STRUCTURE (Prichard et al. 2000) was used to determine the number of groups; the individual was the unit of analysis. The 13 nuclear introns were formatted as single-nucleotide polymorphism (SNP) (Manthey et al. 2011; Walstrom et al. 2012). Individuals (n = 60) represented by two or more loci were used; 39 individuals were from the Asian haplogroup in the mtDNA tree, 14 from the European clade and seven from the Caucasus (Supporting information Table S1.1). The STRUCTURE analyses assumed an admixture model, correlated allele frequencies, and a fixed lambda value (which was inferred by setting K = 1 and allowing lambda to be estimated in an initial analysis). We analyzed the data for K

= 1 to 10 with five replicates for each value of *K*. Each run contained 100,000 steps as burn-in followed by 1 million steps. The Δ*K* was calculated *ad hoc* (Evanno et al. 2005) and used to identify the best estimate of *K*. DISTRUCT (Rosenberg 2004) was used to produce figures from the STRUCTURE output.

Second, Evolutionary Analysis Sampling Trees (*BEAST; Heled and Drummond 2010) was used to reconstruct a population tree (sampled localities were the analytical units) to identify population structure based on multiple nuclear genes. Although *BEAST is designed for estimating species trees, we used this program because (1) gene flow between populations may influence the estimate of divergence times or population sizes (Busch et al. 2011), but should not mislead the group delimitation of populations, (2) other studies have used this program to analyze phylogenetic relationships of populations, some of which were not reciprocally monophyletic for mtDNA or other gene trees, or had inter-population gene flow (e.g., Tavares et al. 2010; Busch et al. 2011), and (3) our analyses based on different numbers of loci and sampled localities returned convergent results (see the Results) and thus we believe that the application of this program to group delimitation is valid. Because *BEAST requires each taxon (sampling locality in this case) to have at least one allele in each gene and the 13 introns were unevenly sampled, we adopted three datasets with different combinations of numbers of loci and localities, which were (1) 13 introns × 10 localities, (2) 5 introns × 16 localities and (3) 2 introns × 21 localities. For the first dataset, five localities were in the Asian mtDNA haplogroup, four in the European one and one in the Caucasian one; for the second dataset, 11 were in the Asian haplogroup, four in the European one and one in the Caucasian one; for the third dataset, 15 were in the Asian haplogroup, five in the

European one and one in the Caucasian one (see Supporting information Table S1.1 for detailed information). To evaluate the effect of Z-linked loci, two analysis based on the same datasets of 13 introns × 10 localities and 5 introns × 16 localities but omitting Z-linked loci were conducted. Unlinked substitution models based on Modeltest 3.7 estimates were assigned to each of the 13 genes, gene-specific mutation rates were allowed, and a strict clock model was assumed for each gene. Due to its high-resolution in the gene tree analysis (see the Results), the relative mutation rate of ACO-I15 gene was set as 1.0 so that branch lengths were scaled in units of substitution per site of the ACO-I15 gene (Kubatko et al. 2011). Each *BEAST analysis included a MCMC chain of 100-300 million steps, sampled every 10,000 steps, and the first 10% of the steps were discarded as burn-in. Trace plots were checked using TRACER v 1.5 (Rambaut and Drummond 2007) to assess convergence in MCMC analyses and three independent runs were performed to assure convergence in tree estimates.

Species tree estimation

We used *BEAST to explore the phylogeny among the three haplogroups defined by mtDNA, using the multilocus data from all available samples (Table 1.1) except for one individual that was assigned to one group based on mtDNA tree and another based on the STRUCTURE analyses and multilocus population trees (see the Results). The analytical unit was the mtDNA haplogroup. This approach allowed us not only to use the whole dataset but also to estimate the posterior probabilities for all three possible phylogenetic topologies. To evaluate the signal from the mtDNA data, we prepared two datasets for analyses, one contained all the 14 loci (mtDNA and 13 nuclear introns) and the other contained only the 13 introns. The program was run using the same conditions as those in

the population tree analysis except that additional analyses assuming a relaxed uncorrelated lognormal clock model for each gene were conducted.

Likelihood ratio tests for species tree topologies

We modified Carstens and Knowles' (2007) coalescence-based likelihood ratio tests to assess whether a particular species tree topology was significantly better than others (including a trichotomous topology). The computation process involved: (1) estimating a maximum likelihood (ML) gene tree for each locus using the RAxML web server (http://phylobench.vital-it.ch/raxml-bb/index.php; Stamatakis et al. 2008), (2) estimating the probability of each gene tree for a specific species tree using the coalescence-based program STELLS (Wu 2012), (3) calculating the log-likelihood of each species tree from the product of the gene tree probabilities for a given species tree, and (4) using likelihood ratio tests to assess whether the most likely species tree was significantly better than the suboptimal species trees after accounting for multiple comparisons with a Bonferroni correction.

For the ML gene tree estimation, we included only one allele for each (unique) haplotype in the dataset; however, if a haplotype was shared by individuals from two or three groups (i.e., the mtDNA haplogroups), we included one allele per group for the haplotype. The reduction in sample sizes facilitated the calculation of gene tree probabilities and avoided extremely low probabilities due to large numbers of tips in gene trees (J. H. Degnan, personal commun.) without resulting in misleading gene tree topologies. For the two loci with large numbers of haplotypes (i.e., mtDNA with 51 haplotypes and TGFB2-I15 with 44 haplotypes), we randomly picked 25 haplotypes to estimate gene trees three times and used the geometric mean of the three gene tree

probabilities for log-likelihood calculation. The individual branch lengths of species tree defined by STELLS are the numbers of generation divided by 2 N_e (for autosomal genes, but 1/2 N_e for mtDNA and 3/2 N_e for Z-linked genes). The STELLS algorithm allows searching for the branch lengths that maximize the likelihood of a specific species tree topology given the gene trees (with the same ploidy), and thus can solve the problem of manually examining a large tree space in Carstens and Knowles' (2007) approach (Wu 2012). Before computing the probabilities of the 14 gene trees at the second step mentioned in the last paragraph, we used STELLS to find the branch lengths with the highest support based on the 10 autosomal genes (i.e., not including TGFB2-I15, the two Z-linked loci and mtDNA) for the three species tree topologies, ((Asia, Europe), Caucasus), ((Asia, Caucasus), Europe) and ((Europe, Caucasus), Asia), with an initial total tree depth of 0.5 and an initial internal branch length of 0.1. The purpose here was not to find the best species tree but species trees with branch lengths close to the optimal ones, allowing reliable likelihood ratio tests. The branch lengths of the trichotmoous species tree, (Asia, Europe, Caucasus), were obtained by averaging those of the three bifurcating species trees (see Supporting Information Fig. S1.1) and enforcing the internal branch length as 0. The branch lengths of species trees were re-scaled according to ploidy when computing the mtDNA and Z-linked gene tree probabilities.

Demographic History

The program IMa (Hey and Nielsen 2007) was used to estimate the effective population sizes of two current populations and their common ancestral population (θ_1, θ_2, and θ_a, respectively; $\theta = 4N_e\mu$), migration rates (m_1 and m_2; $m = m/\mu$), and divergence times ($t = t\mu$) between haplogroups. All estimated parameters in IMa are scaled to the substitution

rate, μ. A minimum of two independent analyses of > 2×10^7 steps after a burn-in of 10^6 steps were performed for each pairwise comparison. Plots of trend lines and the effective sample size values (ESS > 250) were examined to assess convergence in parameter estimates. Also, at least two independent analyses were performed and compared with each other to assure convergence. To convert the scaled divergence time to real time, we calculated the geometric mean of the substitution rates of these 14 loci by multiplying the sequence lengths by 4×10^{-8} substitutions/site/year for ND2 (Arbogast et al. 2006; we also used a widely used rate for avian mtDNA, 1×10^{-8} substitutions/site/year, see Lovette 2004; Weir and Schluter 2008), 1.35×10^{-9} substitutions/site/year for autosomal introns (Ellegren 2007), and 1.62×10^{-9} substitutions/site/year for Z-linked introns (given the mean divergence of Z-linked introns between chicken and turkey is 1.2 time higher than that of autosomal introns; Ellegren 2007). The IMa analyses were applied to all available individuals and loci (Table 1.1). Analyses based only on the 13 introns were also performed to avoid potential bias introduced by the completely sorted mtDNA sequences (see Google groups of Isolation with Migration, http://groups.google.com/group/isolation-with-migration/, Jan 24, 2007). IMa2 (Hey 2010), which allows multiple populations to be analyzed simultaneously, was deemed not useful for this study due to the uncertain topology for the three haplogroups (see Supporting information for additional IMa2 analyses).

Results

Gene Diversity and Neutrality

We obtained sequence data for 12 to 72 individuals for 11 autosomal and two Z-linked introns (Table 1.1). The 13 introns were located on 10 different chromosomes, including

two on the Z chromosome (Table 1.1). Nucleotide diversity (π) estimates of the 13 nuclear loci ranged from 0.0012 to 0.0079 (mean = 0.0048), all of which were smaller than that for mtDNA (0.015). The mutation rate scalars estimated by IMa for these nuclear loci ranged from 0.283 to 1.722, and were smaller than that for mtDNA (11.965). Theta (Nei 1987) for the Asian phylogroup was the largest (0.0094 in mtDNA and 0.0061 ± 0.0029 [SD] in nuclear genes), followed by the European group (0.0029 in mtDNA and 0.002 ± 0.0016 in nuclear genes) and the Caucasian group (0.001 in mtDNA and 0.001 ± 0.0012 in nuclear genes; Table 1.1). To evaluate the effects of differing sample sizes among the three groups, we randomly sampled the same numbers of individuals as those in the Caucasian group from the Asian and European groups three times. Estimates of θ showed the same relative ranking (0.0048 and 0.0024 in mtDNA and 0.0054 ± 0.0026 and 0.0024 ± 0.0018 in nuclear genes for the Asian and European groups, respectively). Seven of 13 introns contained one to three indels, which ranged from one to 14 bp (Table 1.1). No intra-locus recombination was detected in the 13 introns. Seven loci (ND2, ACO-I15, TGFB2-I5, RHO, 17483, 13380, and 12021) containing 5 or more individuals for each phylogroup were included in the HKA tests. The multilocus HKA tests could not reject the neutral model in all pairwise comparisons among the three phylogroups (P = 0.62, 0.79, and 0.94; 10,000 permutations) and the comparison between the three phylogroups combined and *S. e. arctica* (P = 0.23; 10,000 permutations).

MtDNA and Nuclear Gene Trees

The mtDNA haplotype network revealed three distinct haplogroups separated from one another by 29 and 32 mutational steps (Fig. 1.1b). In the Asian group, most haplotypes radiated from one common haplotype by one to four mutation steps, except for one

haplotype from Japan that was separated from the common one by 11 mutation steps. The same three haplogroups were also revealed in the neighbor-joining tree (Zink et al. 2006) and the Bayesian consensus tree (not shown). However, the relationship among the three mtDNA haplogroups in the neighbor-joining and Bayesian trees appeared to be a trichotomy with low support for the short internal branch. The networks and Bayesian consensus trees (not shown) for each nuclear gene were not geographically structured except for three loci, ACO- I15, ABCA1, and 14783 (Supporting information Fig. S1.2). The networks and gene trees for these three loci showed to some extent geographic structure corresponding with the Asia-Europe-Caucasus pattern (Supporting information Fig. S1.2). Two of these three loci, ACO-I15 and ABCA1, are Z-linked.

Group Delimitation using Multiple Nuclear Genes

The STRUCTURE analyses showed that three-group structure has the highest support based on ΔK (Fig.1c and Supporting information Fig. S3; all individuals had estimated membership coefficients [Q] > 0.99 expect for two with Q = 0.98 and one with Q = 0.83). These groups matched the mtDNA tree except for one individual from Vyatka, which was assigned to the Asian group on the mtDNA tree but to the European group in the STRUCTURE analyses (Fig. 1.1). A two-group pattern (Asia and Europe plus Caucasus) had the second highest support based on ΔK (see Supporting information Fig. S1.3 and S1.4).

The *BEAST population trees based on the three datasets with different combinations of numbers of loci and localities all recovered the three mtDNA phylogroups (i.e., Asia, Europe, and Caucasus) (Fig. 1.2a, 1.2b and 1.2c). The Vyatka individual was assigned to the European group (Fig. 1.2b and 1.2c) as in the

STRUCTURE analyses. The population trees had low posterior probabilities for the internal node leading to the Asian and European groups (Pp = 0.68, 0.56 and 0.8). The two analyses (not shown) omitting Z-linked loci recovered the same population trees as those based on the original datasets.

Multilocus Phylogenetic analyses of MtDNA Phylogroups

The species trees did not support a bifurcating pattern among the three mDNA haplogroups (Fig. 1.2d). The species trees based on the 13 introns or 14 genes (mtDNA and 13 introns), assuming a strict clock or a relaxed uncorrelated lognormal clock model, all had low posterior probabilities for a sister-group relationship between the Asian and European groups ranging from 0.64 to 0.73 and a relatively short internal branch compared to the terminal branches (Fig. 1.2d). Although the posterior probabilities for the internal nodes leading to the Asian and European groups were higher than those for the other two possible topologies (ranging from 0.27 to 0.1 for the datasets with the 13 introns or 14 genes and a strict or relaxed clock model), they were smaller than 0.95 (the threshold for confident inferences in Bayesian-based trees; Alfaro et al. 2003). Therefore, these results suggested that the three groups diverged from one another during a relatively short period of time if not simultaneously.

Likelihood ratio tests for species tree topologies

Although the species tree topology of ((Asia, Europe), Caucasus) had the highest likelihood, the likelihood ratio tests showed that this tree topology was not significantly better than the trichotomous tree or the other two bifurcating topologies (Table 1.2). Thus, a trichotomous divergence history among these three groups could not be rejected, which was consist with the *BEAST analyses.

Demographic History

The IMa analyses (based on mtDNA and 13 introns) showed that the effective population sizes (θ) of these three haplogroups were statistically different from one another as their 95% CIs did not overlap (Fig. 1.3a, 1.3c, and 1.3e): the Asian group (6.77, 95% CI = 5.29 - 8.97) was the largest, the European group (1.17, 95% CI = 0.81 - 1.76) was second largest, and the Caucasian group (0.32, 95% CI = 0.16 - 0.64) was the smallest. The Asian group was statistically larger than its ancestral population (0.96, 95% CI = 0.20 - 3.29), whereas the effective population sizes of the other two groups were not statistically different from their ancestral populations (Fig. 1.3a, 1.3c, and 1.3e). The analysis suggested that there has been a low level of gene flow between the European and Asian groups since divergence (Fig. 1.3b). The converted migration rates (N_em) were 0.07 individual per generation (95% CI = 0.02 - 0.21) from the Asian to European group and 0.38 individual per generation (95% CI = 0.17 - 0.83) from the European to Asian group. There was no gene flow in other comparisons (Fig. 1.3d and 1.3f), or the posterior distribution of the migration rate did not allow us to reject zero (i.e., the migration rate from the Asian to Caucasian group in Fig. 1.3d). The divergence times of the three comparisons were not statistically different from one another because their CIs overlap considerably (Fig. 1.3g). The converted divergence times (using the lower substitution rate, 1×10^{-8} substitutions/site/year, for the mtDNA data) were 1,800,000 years (95% CI = 1,060,000 – 2,510,000 years) between European and Asian groups, 1,510,000 years (95% CI = 700,000 – 2,200,000 years) between Caucasian and Asian groups, and 1,140,000 years (95% CI = 680,000 – 1,880,000 years) between Caucasian and European groups. These estimates using the higher mtDNA substitution rate (1,260,000 to

2,000,000 years, the peak values of posterior distributions of the three comparisons; 4×10^{-8} substitutions/site/year for the mtDNA substitution rate) were similar to those using the lower rate. The IMa estimates based solely on the 13 introns suggested a similar history to that based on mtDNA plus the 13 introns. The CIs of the divergence times of the three comparisons based on the 13 introns (Fig. 1.3h) overlap more than those based on mtDNA plus the 13 introns (Fig. 1.3g). The range of divergence times based on the 13 introns was from 1,080,000 to 1,580,000 years (the peak values of posterior distributions).

Discussion

Patterns of Selection and Genetic Variation of MtDNA and Introns

Several authors suggest that mtDNA is biased by natural selection and that evolutionary inferences based on mtDNA are flawed (e.g., Dowling et al. 2008; Galtier et al. 2009). Zink et al. (2006) specifically addressed the question of selection acting on mtDNA sequences of nuthatches, and concluded that some substitutions were slightly deleterious, but the overall phylogeographic pattern was not obscured by (purifying) selection. Because neutrality tests based on single loci suffer from the confounding effect of demographic change (Ballard and Whitlock 2004), which is the case in nuthatches, we used a more sophisticated method, the HKA test, to compare multiple genes in this study. The HKA tests showed no evidence of selection on the mtDNA and the nuclear introns. Therefore, the patterns of genetic variation of the mtDNA and introns are dominated by the joint effects of genetic drift and gene flow rather than natural selection.

The observed differences in genetic diversities between the mtDNA and introns reflect their neutral evolutionary rates (Kimura 1968, 1969). The genetic diversities of introns were 2 to 10 (mean = 3) times lower than that for mtDNA. The differences in the mutation rate scalars, indicating relative mutation rates of genes from IMa, between mtDNA and introns were even larger (Table 1.1). Although the mutation rate scalars depend on the lengths of genes (because IMa defines mutation rate on a per-locus, not per nucleotide, basis; Hey and Nielsen 2004), which were about twice as long on average for ND2 than for these introns (Table 1.1), the differences in the mutation rate scalars between ND2 and introns were more than two times larger. Consequently, the results indicate that the substitution rate of ND2 is higher than introns in Eurasian nuthatches, which is concordant with other reports (Arbogast et al. 2006; Ellegren 2007), although a few exceptions have been observed (e.g., Bensch et al. 2006).

Patterns of Variation and Coalescence Time

Most nuclear gene trees, except for the sex-linked ones, did not recover the three groups observed in the mtDNA gene tree. Other multilocus studies reported that mtDNA trees reached reciprocal monophyly whereas nuclear gene trees had not (e.g. Dolman and Moritz 2006; Lee and Edwards 2008), although a few exceptions have been reported (e.g., Brelsford and Irwin 2009). These observations are consistent with the positive relationship between coalescence times and the N_e of loci with different modes of inheritance (see Palumbi et al. 2001; Hudson and Coyne 2002). For example, the three-times rule (Palumbi et al. 2001) as well as other theoretical studies (Maynard Smith 1987; Birky 1991) state that under neutrality, most autosomal genes (> 50%) will be monophyletic when divergence time exceeds 4 N_e whereas mtDNA reaches reciprocal

monophyly when divergence time is 1 N_e (or 2 N_{ef} assuming a 1:1 sex ratio). Based on the same rationale, we can predict that most Z-link genes will be monophyletic when divergence time is larger than $3N_e$. However, other studies have indicated that the stochasticity of the coalescence process, population structure, or changes in population size can result in deviations from the three-times rule. Hudson and Turelli (2003) used simulations (ignoring population changes and structure) to show that the divergence time for most nuclear genes (> 50%) exhibiting monophyly can be 2-3 times longer than the three-times rule predicts.

In this study, the divergence times were 16.1, 4.6, and 0.9 N_e (averaging the pairwise comparisons from IMa) for the Caucasian, European, and Asian groups, respectively. This explains why the Caucasian and European groups were on long branches in the mtDNA neighbor-joining tree in Zink et al. (2006; their Fig. 4), whereas the Asian group was reciprocally monophyletic but with a shorter branch. According to the three-times rule, the Caucasian and European groups should exhibit monophyly in most autosomal and Z-linked genes, whereas the Asian group is less likely if at all to exhibit monophyly for nuclear loci. According to Hudson and Turelli (2003), only the Caucasian, but not European or Asian, group should exhibit monophyly in most nuclear genes. Our results are more consistent with Hudson and Turelli's (2003) predictions than the three-time rule, *sensu stricto*. For example, nuclear alleles from the Caucasus usually tend to be clustered together, but the European group rarely reached monophyly for autosomal genes (Supporting information Fig. S1.2).

The fact that Z-linked genes were more geographically structured than autosomal genes supports the logic of the three-time rule (i.e., coalescence times are positively

related to N_e of genes), although not its quantitative prediction. Other possible causes for the higher geographically structured Z-linked genes than autosomal genes are (1) higher variance in male reproductive success (Barker et al. 2008), (2) female-biased dispersal, or (3) reduced gene flow in sex-linked genes because of Haldane's rule (Carling and Brumfield 2008). Although known as a socially monogamous bird, extra-pair breeding has been reported in *Sitta europaea* (Segelbacher et al. 2005), and the resulting higher variance in male reproductive success might reduce the N_e of Z-linked genes more than autosomal ones (Nunney 1993; Barker et al. 2008). Therefore, the coalescence rate of Z-linked genes could be higher than the expectation based solely on their ploidy. Second, females are the dispersing sex in most passerine birds (Clarke et al. 1997) and the resulting female-biased dispersal (i.e., male philopatry) can increase geographic structure in Z-linked genes. However, the estimated gene flow levels among these nuthatch groups (0.07 and 0.38 individuals/generation between the Asian and European groups, and zero between the other two comparisons) were too low to prevent differentiation by drift (Crow and Kimura 1970; Slatkin 1987). Thus, female-biased gene flow is unlikely to explain the different level of geographic structure between the Z-linked and autosomal genes in nuthatches. Finally, Haldane's rule (Haldane 1922) predicts limited gene flow in sex-linked genes due to sex-skewed hybrid incompatibility, but it only applies to partially reproductively isolated taxa. We do not have information regarding the level of reproductive isolation among these nuthatch groups. Therefore, the third hypothesis is not testable in this case. Therefore, we think that the smaller N_e of Z-linked genes due to smaller ploidy and/or higher variance in male productive success leads to their higher geographical structure.

Despite little or no geographic structure in many nuclear gene trees, the population trees based on the nuclear genes combined revealed the same phylogeographic pattern as did the mtDNA gene tree. Thus, the three mtDNA groups of Eurasian nuthatches define valid taxa. We believe that the lack of geographic structure shown by most of the autosomal loci is due to their longer coalescence times, not a pattern of male-mediated gene flow, which is supported by the fact that Z-linked genes showed higher levels of geographic structure than the autosomal introns.

Multilocus versus MtDNA Phylogenetics of the Eurasian Nuthatch

The phylogenetic trees based on mtDNA alone, the 13 introns alone, or mtDNA plus the 13 introns had low support for the (short) internal branch. Although the *BEAST species trees had higher support for the sister relationship of the Asian and European than the other two possible alternatives, the posterior probabilities (0.64 to 0.73) were not high enough for confident inference (Alfaro et al. 2003) and the STRUCTURE analyses revealed an alternative history that the Asian group split first from the other two groups (when K= 2, Supporting information Fig. S1.4). Furthermore, the likelihood ratio tests based on the 14 genes could not reject the trichotomous species tree topology. These results indicate that the three groups separated from one another closely in time, which was suggested by the mtDNA gene tree (Zink et al. 2006). Similarly, the posterior probability distributions of divergence time estimates between these groups overlapped with one another considerably. Thus, the IMa analysis was consistent with the inference of temporally close or a simultaneous origin(s) of the three groups.

Comparison of Demographic Inferences Based on MtDNA Versus Nuclear Loci

The mtDNA gene tree, with deeply reciprocally monophyletic groups, suggests no recent gene flow among the three groups, coinciding with the STRUCTURE results. However, IMa estimated low gene flow levels between the Asian and European groups (0.07 and 0.38 individuals/generation). We argue that the IMa estimates of gene flow could be exaggerated by (1) the input from the Vyatka individual, (2) a low level of homoplasy in the introns given that reticulations are common in the haplotype networks of these introns (Supporting information Fig. S1.2; Bandelt et al. 1999), or (3) poor fit of substitution models available in IMa to the data (Strasburg and Reiseberg 2010). We conducted two additional IMa analyses based on the data excluding (a) the Vyatka individual and (b) the Vyatka individual plus two introns with the most reticulated haplotype networks (i.e., TGFB2-I5 and RHO). The posterior probability distributions moved towards zero and included the probability of zero in the two additional IMa analyses although their peaks were still larger than zero (Supporting Information Fig. S1.5). Therefore, the first two hypotheses can at least partially explain the apparently conflicting estimates of gene flow between the mtDNA tree and nuclear-based IMa analyses. The third hypothesis is difficult to test without a greater array of substitution models in IMa. By contrast, we cannot rule out an alternative hypothesis that mtDNA is a less sensitive indicator of gene flow than nuclear genes. The lower absolute numbers of immigrating genes in mtDNA compared with autosomal genes (i.e., only females transmit mtDNA whereas both male and female immigrants carry two copies of autosomal genes) can make the former less sensitive to gene flow especially at a level of smaller or equal to one individual per generation, which is sufficient to prevent

population differentiation regardless of population size (Crow and Kimura 1970; Slatkin 1987).

Analyses of mtDNA data suggest the same relative rankings of effective population sizes for the three phylogroups as do the multiple nuclear genes. That is, the Asian phylogroup was the largest, the European group was the second largest, and the Caucasian group was the smallest (Table 1.1, Fig. 1.3). IMa analyses suggest that the Asian group experienced dramatic population expansion since divergence, whereas the other two groups did not. The star-like cluster of mtDNA haplotypes, detected in the Asian group but not in the other two groups (Fig. 1.1b), is consistent with the IMa analyses suggesting population expansion in the former group. The multilocus IMa analyses based solely on nuclear data suggest that the three phylogroups separated from one another 1 to 1.6 million years (Ma) ago. MtDNA sequence divergence between the three phylogroups ranges from 0.0287 to 0.0384 substitutions/site. If we use the substitution rate of 1×10^{-8} substitutions/site/year (Lovette 2004; Weir and Schluter 2008), the divergence times range from 1.44 to 1.92 Ma ago, which are similar to the nuclear-based IMa estimates. However, if we apply the substitution rate of 4×10^{-8} substitutions/site/year (Arbogast et al. 2006) to the ND2 data, the divergence times range from 0.36 to 0.48 Ma ago, which are much younger than the nuclear-based IMa estimates. The higher substitution rate may be only applicable to the relatively recent events, e.g., < 1 Ma ago, which are less likely to be influenced by purifying selection and sequence saturation (Ho et al. 2005; Arbogast et al. 2006). Nonetheless, this suggests caution in interpreting ages of divergence based solely on mtDNA.

Estimates of divergence time and population expansion derived from mtDNA are generally consistent with those suggested by the nuclear loci in this study. However, multilocus data help quantify demographic parameters because the CI of estimates decreased as the numbers of loci used increased (Supporting Information Fig. S1.6 and Table S1.2; also see Lee and Edwards 2008). In addition, comparing mtDNA and nuclear genes is useful to identify introgression (Bossu and Near 2009). For example, the individual from Vyatka, located between the Asian and European groups, was assigned to the former in the mtDNA tree but to the latter in the *BEAST population trees and STRUCTURE estimates based on multiple nuclear genes (Fig. 1.1). Given the long branches of the Asian and European groups in the mtDNA tree and the multilocus population trees, we believe that this conflicting pattern was a result of recent but infrequent immigration rather than incomplete lineage sorting. However, more samples from this area are required for detailed analyses of introgression, which is beyond of the scope of this present study.

There have been at least eight glacial periods during the past 2 million years (Gibbard and Van Kolfschoten 2004), each of which also contained several glacial-interglacial cycles (Svendsen et al. 2004; Lisiecki and Raymo 2007). Thus, the changes in population sizes and distribution ranges of the three groups were likely more dynamic than can be detected with these data and methods. Nevertheless, the results characterize the main trend in the phylogeographic history of nuthatches as a (nearly) three-way split occurring during the early or middle Pleistocene (1-2 Ma ago; Head et al. 2008), a negligible level of gene flow if at all between the Asian and European groups, and isolation of the Caucasus, and more recent population expansion in the Asian group. An

interesting yet unanswered question is how these three groups have remained separate from another one over several glacial cycles during which their ranges could separate and connect repeatedly.

Taxonomy and Implications for the speciation process

The mtDNA and nuclear data suggest the existence of three taxa within the Eurasian nuthatch. Any phylogenetic analysis or conservation assessment that requires knowledge of independently evolving taxa should use the three taxa confirmed in this study rather than considering the species as a single unit. We suggest that these three taxa are phylogenetic species, and likely biological species. However, we suggest that taxonomic changes are not yet warranted, pending analysis of the remainder of the range. For example, our preliminary analyses suggest additional taxa in eastern Asia.

Most students or models of the evolutionary process assume that population divergence is a dichotomous process. Many analyses of mtDNA have suggested multiple contemporaneous splits (e.g., Salzburger et al. Marmi et al. 2006; Pastene et al. 2007; Klicka et al. 2011), but with only a single gene tree, strong inferences are not possible. In the Eurasian nuthatch, our survey of nuclear loci confirms the inference from mtDNA that a single lineage split into three taxa simultaneously or during a short period of time. Although adding more genes might resolve the trichotomy, it is possible that the groups separated from one another during the same geographic event such as one glacial advance. If this phenomenon is confirmed in other lineages, it will imply that bifurcation is not the only mode for diversification.

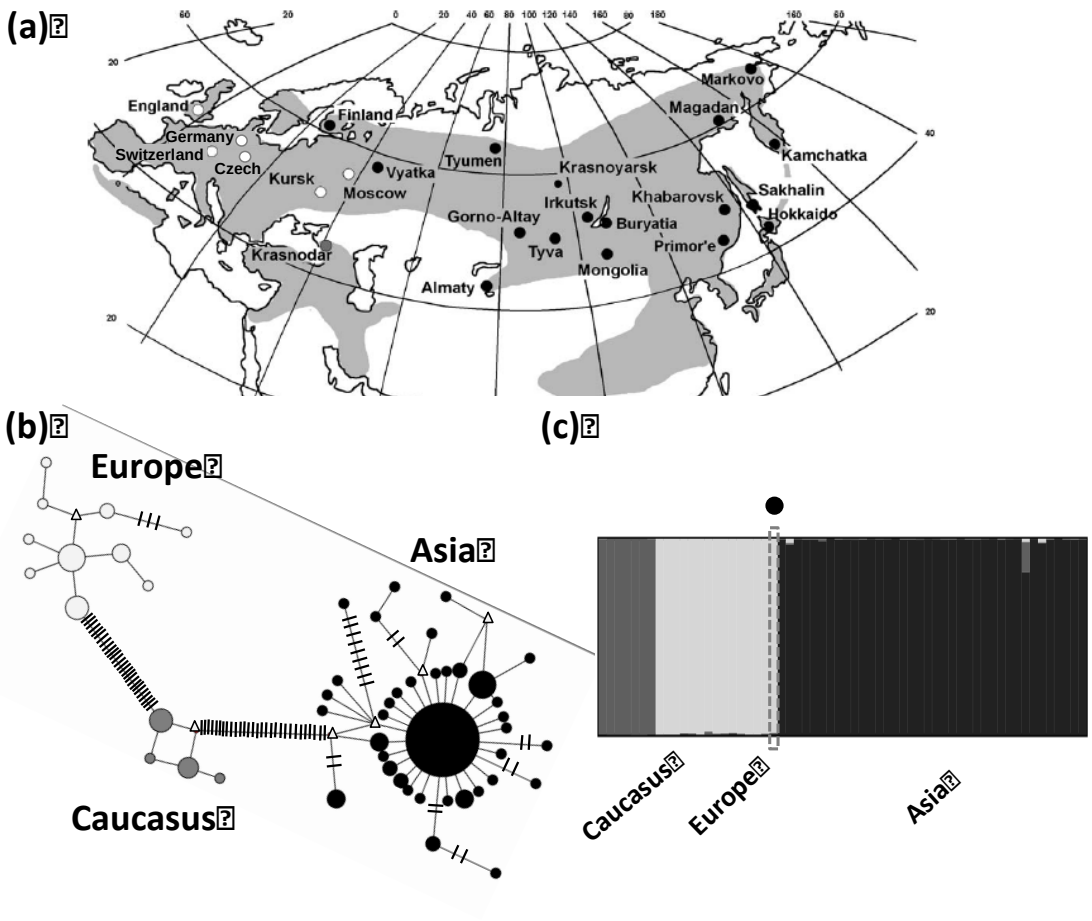

Figure 1.1. (a) Breeding range of the Eurasian nuthatch *Sitta europaea* and location of sample sites (from Fig. 1 in Zink et al. 2006). Black circles indicate sample sites in the Asian clade, white circles indicate those in the European clade, and the gray circle indicates that in the Caucasian clade. (b) Network of mtDNA haplotypes constructed using the minimum spanning criterion. Colors of circles on the network indicate the clades corresponding to those in (a). Open triangles indicate unsampled or extinct haplotypes. Sizes of circles are proportional to haplotype frequencies. Short lines indicate one mutation step. (c) STRUCTURE results was shown when $K = 3$ and colors of vertical columns, indicating individual samples, corresponding to those in (a). The black circle in (c) indicates the individual from Vyatka assigned to the European group in the STRUCTURE analyses but to the Asian group in the mtDNA network.

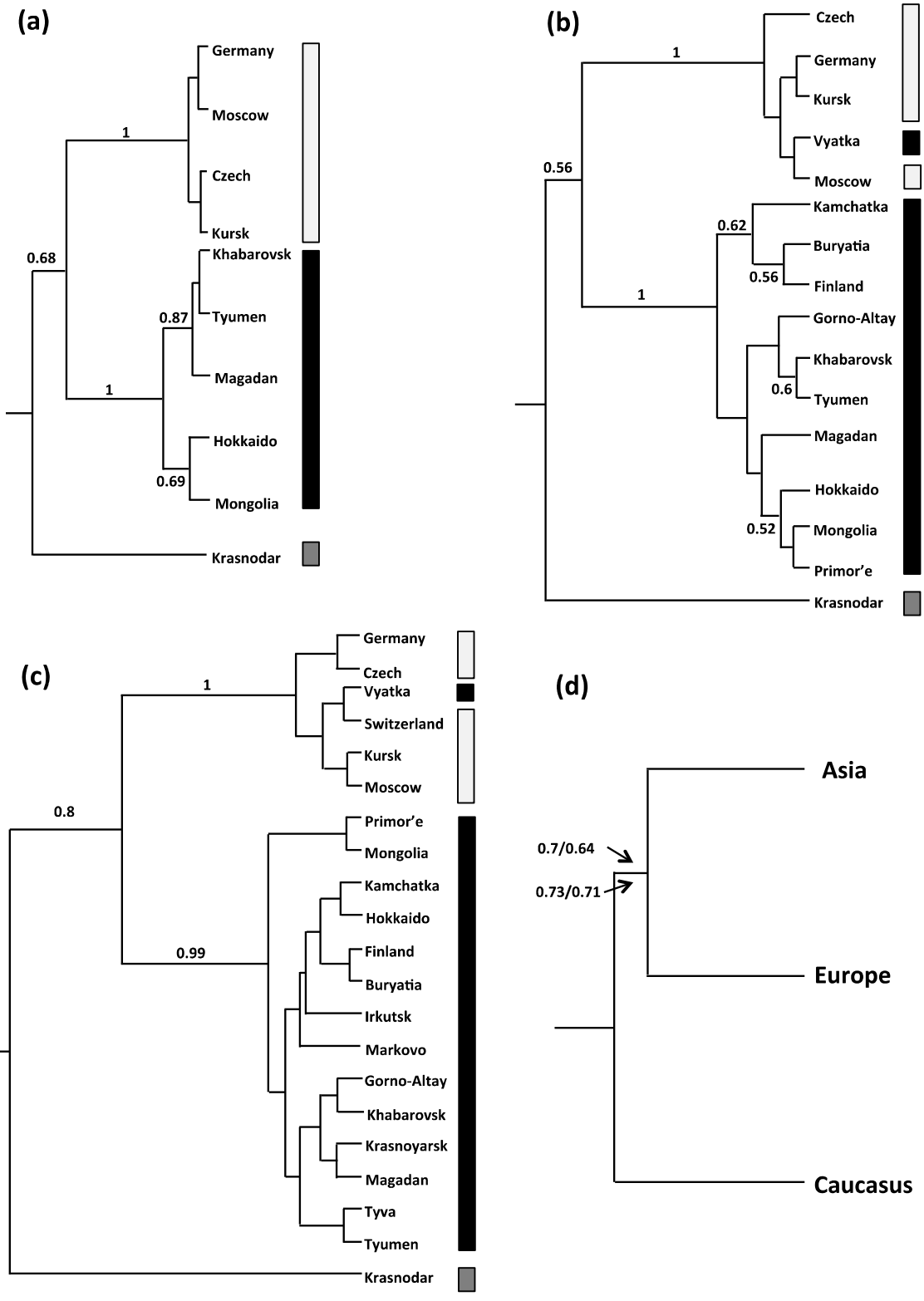
(a)
Germany
Moscow
Czech
Kursk
Khabarovsk
Tyumen
Magadan
Hokkaido
Mongolia
Krasnodar
1
1
0.68
0.87
0.69
(b)
Czech
Germany
Kursk
Vyatka
Moscow
Kamchatka
Buryatia
Finland
Gorno-Altay
Khabarovsk
Tyumen
Magadan
Hokkaido
Mongolia
Primor'e
Krasnodar
1
0.56
1
0.62
0.56
0.6
0.52
(c)
Germany
Czech
Vyatka
Switzerland
Kursk
Moscow
Primor'e
Mongolia
Kamchatka
Hokkaido
Finland
Buryatia
Irkutsk
Markovo
Gorno-Altay
Khabarovsk
Krasnoyarsk
Magadan
Tyva
Tyumen
Krasnodar
1
0.8
0.99
(d)
Asia
Europe
Caucasus
0.7/0.64
0.73/0.71

Figure 1.2. Multilocus *BEAST population trees (a, b and c) and species tree (d). Analyses were based on the datasets (a) 13 introns × 10 localities, (b) 5 introns × 16 localities, (c) 2 introns × 21 localities, and (d) 13 introns plus mtDNA and 13 introns from all available samples except for the Vyatka individual. Colors of vertical bars in (a), (b) and (c) corresponding to geographic regions (Fig. 1a) and those in mtDNA network (Fig. 1b). Posterior probabilities (Pp) for the nodes and only > 0.5 are presented above or below branches. In (d), Pp above the internal brach are based on the data of 13intron plus mtDNA with strict clock/relaxed clock model and Pp below the branch are for the data of 13 intron. The trees were rooted with one *S. e. arctica* sample.

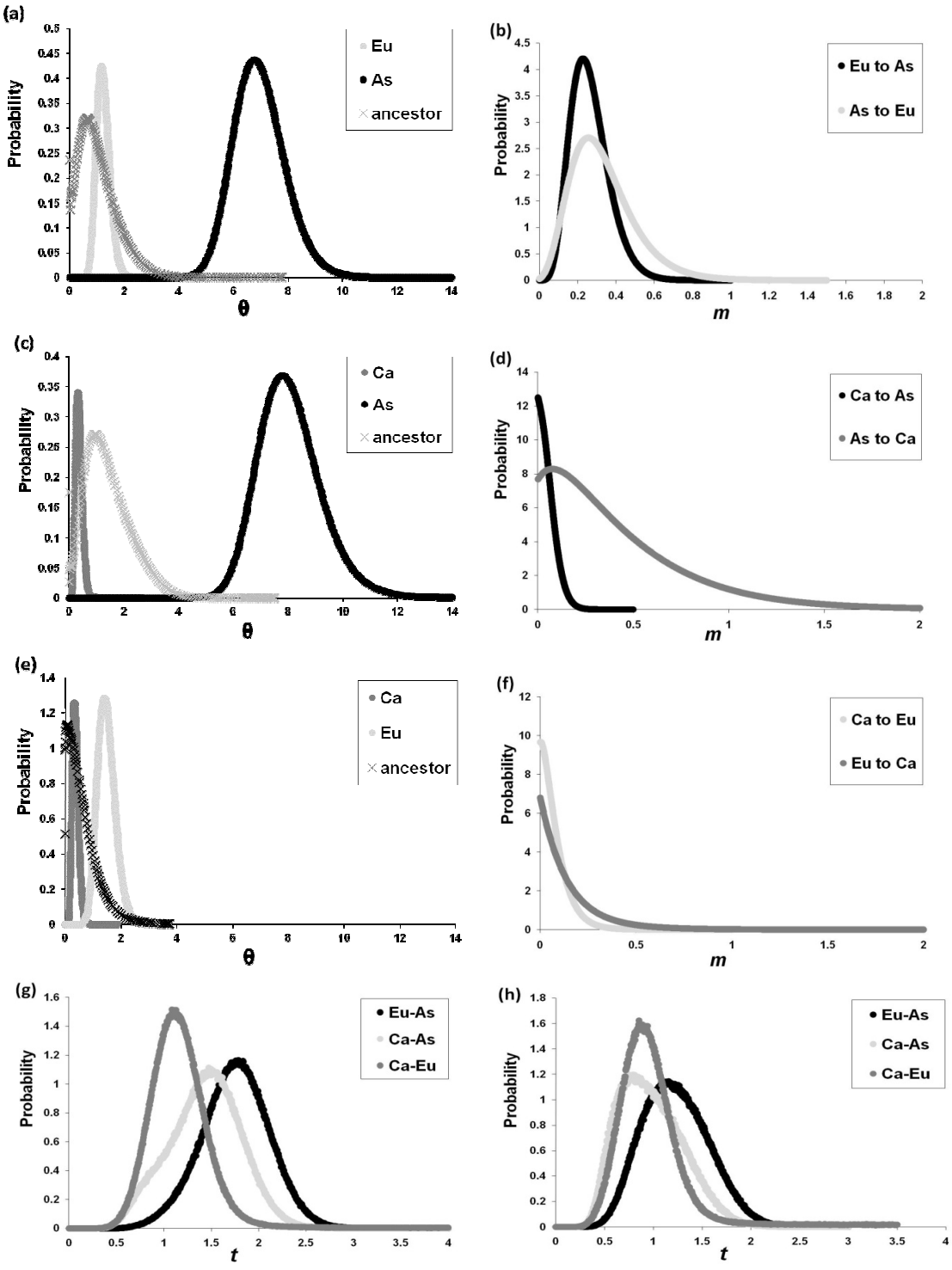
(a)
Probability
θ
Eu
As
ancestor
(b)
Probability
m
Eu to As
As to Eu
(c)
Probability
θ
Ca
As
ancestor
(d)
Probability
m
Ca to As
As to Ca
(e)
Probability
θ
Ca
Eu
ancestor
(f)
Probability
m
Ca to Eu
Eu to Ca
(g)
Probability
t
Eu-As
Ca-As
Ca-Eu
(h)
Probability
t
Eu-As
Ca-As
Ca-Eu

Figure 1.3. The marginal posterior probabilty distribution of the IMa model parameters scaled by the geometric mean of substitution rates of genes, μ. Effective population sizes (θ) of the pairwise comparisons among the Asian (As), European (Eu), and Caucasina (Ca) groups and their ancestral populations are shown in (a), (c), and (e). Migration rates (*m*) in two directions for each pairwise comparsions are in (b), (d), and (e). Divergence times (*t*) of the three pairwise comparsions are in (g). The results above (from a to g) are based on the sequence data from mtDNA (complete ND2 gene) and 13 introns combined. Divergence times of the three pairwise comparsions based on the 13 introns are shown in (h). Note that μ of the mtDNA and 13 introns combined is larger than that of the 13 introns.

Table 1.1. Characteristics of the 14 loci in this study. Chr indicates the chromosome where the gene is located. L indicates the length of the locus used in the analyses. Individual shows the number of individuals sequenced and value within the parentheses indicates the number of individuals in Asia/Europe/Caucasus. Clark / PHASE indicates the number of haplotypes determined by PHASE program followed by Clark's (1990) parsimony algorithm (numerator) and solely by PHASE (denominator). π indicates the nucleotide diversity. $\theta_{(As)}$, $\theta_{(Eu)}$, and $\theta_{(Ca)}$ indicate $4N_e\mu$ of the haplogroups, Asia, Europe, and Caucasus, estimated based on Nei (1987). Mutation rate scalars, estimated using IMa based on the Europe-Asia comparison, indicate the relative mutation rates of the 14 loci with a geometric mean of one. The lengths of indels are listed as they occurred in each locus.

Locus	Chr	L	Individual	Clark / PHASE	π	$\theta_{(As)}$	$\theta_{(Eu)}$	$\theta_{(Ca)}$	Mutation rate scalar	Indel length
ND2	Mt*	1041	136 (102/23/11)	51[#]	0.0154	0.0094	0.0029	0.0010	11.97	
ACO-I15	Z	513	72 (50/15/7)	12/12	0.0059	0.0055	0.0005	0.0007	0.63	
TGFB2-I5	3	476	70 (42/16/11)	42/43	0.0061	0.0099	0.0032	0.0006	1.72	14
RHO	12	847	24 (12/7/5)	21/21	0.0038	0.0054	0.0011	0.0004	1.38	1
17483	4	486	27 (15/7/5)	15/15	0.0056	0.0031	0.0039	0.0022	0.75	2
13380	7	678	26 (14/7/5)	20/21	0.0078	0.0096	0.0042	0	1.60	5, 8, 1
12021	24	691	25 (14/6/5)	17/17	0.0052	0.0056	0.0029	0.0005	1.09	
08352	5	378	12 (5/4/3)	9/9	0.0077	0.0075	0.0051	0.0035	0.89	
06635	6	559	12 (5/4/3)	6/6	0.0056	0.0079	0.0014	0.0024	1.21	12, 4, 5
01304	11	685	12 (5/4/3)	11/11	0.0052	0.0052	0.0017	0	1.15	1
09385	20	313	12 (5/4/3)	7/7	0.0038	0.0045	0.0037	0.0028	0.28	
11074	20	392	12 (5/4/3)	11/11	0.0012	0.0108	0.0030	0	1.36	
14765	3	799	12 (5/4/3)	5/5	0.0013	0.0022	0.0005	0	0.44	2, 1
ABCA1	Z	365	12 (5/4/3)	5/5	0.0038	0.0021	0	0	0.40	
				Mean (± SD)†	0.0048 (± 0.0021)	0.0061 (± 0.0029)	0.002 (± 0.0016)	0.0010 (± 0.0012)	0.99 (± 0.47)	

* mitochondrial DNA

[#] number of mtDNA haplotype, not determined by PHASE or Clark's algorithm

† mean (± standard deviation) of values for 13 nuclear genes

Table 1.2. Likelihood ratio tests among four species tree topologies. ln *L* indicates log-likelihood for the given species tree calculated from the product of the probabilities of 14 gene trees. $2\Delta L$ indicates twice the log-likelihood difference between the optimal and the suboptimal topologies. df indicates degrees of freedom. Probability (of chance occurrence) is calculated from χ^2 after correcting for multiple comparisons with a Bonferroni correction. The branch lengths of these species trees are shown in the Supporting information Fig. S1.3.

Species tree topology	ln *L*	$2\Delta L$	df	Probability
((Asia, Europe), Caucasus)	-469.105	0		
((Europe, Caucasus), Asia)	-469.713	1.216	1	> 0.05
(Asia, Europe, Caucasus)	-470.610	3.010	1	> 0.05
((Asia, Caucasus), Europe)	-471.481	4.752	1	> 0.05

Chapter 2

Distinguishing between bottlenecks and selection in the mitochondrial DNA genomes of two Old World flycatchers (*Ficedula parva* and *F. albicilla*)

Hung, C.-M. (in revision)

Determining the underlying mechanisms of genetic diversity has attracted considerable attention in evolutionary biology. The purpose of this study is to assess whether demographic or selective factors caused drastically lower genetic variation in the mitochondrial DNA (mtDNA) ND2 gene of a widely distributed Palearctic flycatcher, *Ficedula albicilla*, compared with its sister species, *F. parva*. Two other mtDNA regions (Cyt*b* and COI) were sequenced to confirm the patterns observed in ND2, and 18 nuclear genes were used to estimate the phylogeographic histories of the two species. I accounted for historical demographic changes when using simulations to test for neutrality. I used likelihood ratio tests of hypotheses and models of protein structure to determine if mtDNA was subject to positive selection. Although *F. albicilla*, but not *F. parva*, experienced a recent population expansion perhaps following a historical population bottleneck, this demographic history cannot explain the extremely low mtDNA variation of the former. In fact, the mtDNA variation of both species is inconsistent with neutral expectation. There was mixed evidence for positive selection directly affecting the mtDNA. It is highly likely that demographic fluctuation and selective forces (positive selection or selective sweeps) work in concert to dramatically reduce the mtDNA variation of *F. albicilla*.

Supplementary Material

Supporting tables 2.1-2.3 are available online.

Introduction

Whether the mechanisms underlying observed genetic diversity are neutral or selection-driven has fueled a continuous debate over several decades in evolutionary biology (Hughes 2007; Hahn 2008; Wares 2010). The neutral theory predicts that most genetic variation has no effect on fitness and is positively correlated to the sizes of populations (Kimura 1983). Observations that conflict with this relationship have often been cited as evidence for positive (adaptive) selection (e.g., Bazin et al. 2006; Bensch et al. 2006). However, few studies have explicitly taken into account historical demographic processes when testing for selection.

Reduced genetic variation in a population can be caused by demographic (neutral) factors, selective factors, or both. Demographic events such as population bottlenecks can reduce genetic variation through reducing population sizes and facilitating genetic drift (Nei et al. 1975). Similarly, selective fixation of a beneficial mutation can abruptly reduce genetic variation in the gene or genes linked to the targeted gene via hitchhiking (selective sweeps or genetic draft; Maynard-Smith and Haigh 1974; Gillespie 2000, 2001). Although theoretical work for each of these factors is well developed, disentangling the two confounding factors from empirical data remains challenging.

Impacts of a particular demographic history should be genome wide, whereas selective events are more likely to affect different regions of a genome separately due to recombination (Hudson et al. 1987). Therefore, comparing genetic variation across independent genes can distinguish the two types of factors. However, stochastic coalescence or mutation processes can result in seemingly inconsistent variation among genes even under neutrality (Rosenberg and Nordborg 2002). Thus, comparisons should

take into account such stochasticity to prevent biased inferences (Peters et al. 2012). In addition, it is possible that demographic and selective factors work in concert to tailor genetic variation. Therefore, explicitly dissecting the underlying processes of the observed pattern can reveal a more comprehensive picture.

The mitochondrial DNA (mtDNA) of two sister species of Old World flycatchers, *Ficedula albicilla* (red-throated flycatcher) and *F. parva* (red-breasted flycatcher), provide a useful opportunity to study the confounding effects of demographic and selective factors in shaping genetic variation. Zink et al. (2008) found that 75 *F. albicilla* individuals, sampled from the major breeding range across over 4,500 kilometers, shared the same haplotype for the ND2 gene (Fig. 2.1). On the other hand, they found that 16 *F. parva* individuals shared five ND2 haplotypes. This striking pattern raises the question of whether the different patterns of mtDNA variation are caused by different demographic histories or selection forces. In this study, I present sequence data from two additional mtDNA regions (Cyt*b* and COI), 17 introns, and one exon for both species and utilize coalescence-based approaches, neutrality tests, likelihood ratio tests and protein structure modeling to 1) test whether the evolution of mtDNA departs from neutral expectation by considering demographic history, 2) search for evidence of positive selection on mtDNA and 3) interpret the phylogeographic history of the two species. This study demonstrates that simultaneously considering demographic history of organisms and traces of selection provides a deeper insight to the evolutionary history of genes.

Materials and Methods

Sequence data collection and analyses

I used ND2 sequence data (1041 bp) for 16 *F. parva* and 75 *F. albicilla* from Zink et al.'s (2008) study (all samples were referred to as *F. parva* in that study; NCBI accession numbers EU326696 to 326786) and one *F. parva* from Sweden downloaded from the GenBank (NCBI accession number GU358799). Zink et al. (2008) sequenced ND2 using two pairs of primers, L5215/H6313 and L5215/H1064 (Hackett 1996, Sorenson et al 1999, Drovetski et al. 2004) to attempt to insure the mitochondrial authenticity of the data. I further checked the validity of the ND2 sequences adopting long PCR to amplify about half of mtDNA genome (around 8,000 bp; from ND6 to COI) or around 4,000 bp (from 16S to COI) to further confirm the validation of the ND2 gene (see Supplementary table 2.1 for the detailed information of primers and the protocol for long PCR). The long PCR products were re-amplified using MetL/AsnH (Pereira and Baker 2004a) and sequenced using L5215/H1064/L420 (L420, M. Westberg, personal communication, see Supplementary table 2.1). Cyt*b* was amplified and sequenced using the primers, L14841/H4a (Kocher et al. 1989; Harshman 1996). Cyt*b* of one *F. parva* from Czech Republic was downloaded from the GenBank (NCBI accession number AJ299689). COI was amplified using the primers, L6615m/H8232m (modified from Sorenson et al. 1999 by Hung) with M13 tails (Boutin-Ganache et al. 2001) and sequenced with the M13 tails (see Supplementary table 2.1). I sequenced 15 autosomal and two Z-linked introns (Table 2.1; Friesen et al. 1999; Shapiro and Dumbacher 2001; Primmer et al. 2002; Backstörm et al. 2006, 2008; Kimball et al. 2009) and one exon (MC1R; Table 2.1) for both strands using published primers (MacDougall-Shackleton et al. 2003). Indels (insertions or deletions) were common among the introns, which were useful for

reconstructing (phasing) haplotypes of individuals with multiple heterozygous sites. Phases of sequences containing indels were sorted manually by subtracting chromatogram peaks upstream of the indel in the reverse primer sequences from the double peaks downstream of the indel in the forward primer sequences. This was repeated in the alternative direction and allowed the two haplotypes of a heterozygous individual to be determined (Sousa-Santos et al. 2005; Dolman and Moritz 2006). The lengths of indels could also be determined by this approach. Multi-base indels were collapsed to single-base polymorphisms for further analyses.

Haplotypes of individuals with multiple heterozygous sites were resolved using PHASE 2.1.1 (Stephens et al. 2001; Stephens and Scheet 2005). Homozygous genotypes and genotypes with single heterozygous site or with indels were set as known alleles to improve the performance of PHASE analyses. The phases of some sites could not be estimated confidently at 90% posterior probability. The phases of these ambiguous sites were resolved using Clark's (1990) parsimony algorithm to minimize the total number of haplotypes and singletons in the samples.

Intra-locus recombination rates were estimated using a Bayesian method (Li and Stephens 2003) implemented in PHASE 2.1.1. The background recombination rate and the recombination rates between two polymorphic sites were estimated and portrayed as 5,000 sampled points from the posterior distribution. The factors by which the estimated recombination rates exceed the background rate were calculated, and the upper and lower bounds of 95% credible interval (CI) of these values were recorded. If one or more estimated values were significantly larger than one, it means there has been significant

recombination occurring between the corresponding sites. Otherwise, we assumed that there was no intra-locus recombination within the locus.

I used DnaSP 5 (Librado and Rozas 2009) to compute nucleotide diversity (π; Nei 1987) of each species and nucleotide distance (D; Nei 1987) between the two species for each gene.

Neutrality tests

Hudson-Kreitman-Aguade (HKA) tests (Hudson et al. 1987) implemented in the HKA program (http://genfaculty.rutgers.edu/hey/software) were used to test the neutrality of the mtDNA, introns, and the lone exon. The HKA test examines whether the association between the level of intra-specific polymorphism and inter-specific divergence departs from the expectation of an evolutionarily neutral model for two or more genes. First, the HKA test was applied to all 18 nuclear genes (17 introns and one exon), 17 introns, and 15 introns (excluding two loci each of which had no polymorphism in one species; see results). Second, I applied the HKA test to these nuclear data plus each of the three mtDNA regions (i.e., ND2, Cyt*b*, and COI), respectively. In addition, I applied the above tests to (1) all individuals of both species, (2) all individuals of *F. albicilla* and one *F. parva* (to only test the genes of *F. albicilla*), and (3) vice versa (to only test the genes of *F. parva*). The widely used M-K test (McDonald and Kreitman 1991) was not applied to this study because of the lack of or very little replacement polymorphism in the mtDNA of the two study species.

Demographic and divergence history

The program IMa (Hey and Nielsen 2007) was used to estimate the effective population sizes of two current populations and their common ancestral population (θ_1, θ_2, and θ_a,

respectively; $\theta = 4N_e\mu$), migration rates (m_1 and m_2; $m = m/\mu$), and divergence times ($t = t\mu$) between the two species. All estimated parameters in IMa are scaled to the substitution rate, μ. A minimum of 2×10^7 steps after a burn-in of 10^6 steps were performed for each analysis. Plots of trend lines and the effective sample size values (ESS > 250) were examined to assess convergence in parameter estimates. Also, at least two independent analyses were performed and compared with each other to assure convergence. The IMa analyses were applied to all available individuals for the 17 introns (Table 2.1). To convert the scaled demographic parameters, we calculated the geometric mean of the substitution rates of these 17 loci by multiplying the sequence lengths by 1.35×10^{-9} substitutions/site/year for autosomal introns (Ellegren 2007), and 1.6×10^{-9} substitutions/site/year for Z-liked introns (given the mean divergence of Z-linked introns between chicken and turkey is 1.2 time higher than that of autosomal introns; Ellegren 2007). I assumed the generation times of the two flycatcher species are two years because most male birds do not breed until the red patch shows in the throat or breast after the second year (Mitrus 2006; 2007). Additional IMa analyses were conducted based on the data sets containing (1) the 17 introns plus one exon and (2) 15 introns excluding two introns, each of which fixed in one species.

While IMa can show changes in population size via the comparison of current and ancestral effective population sizes, more complex population dynamics over time cannot be detected by this program due to its simplified model (Rovito 2010). Therefore, I applied the Extended Bayesian Skyline Plot (EBSP) method (Heled and Drummond 2008) implemented in BEAST v1.6.1 (Drummond and Rambaut 2007) to estimate detailed population size changes through time. This coalescence-based method uses

multi-locus data to recover historical population dynamics without relying on parametric models (Heled and Drummond 2008). The data sets used for EBSP analyses were the same as those for IMa analyses. Unlinked substitution models based on jModelTest (Posada 2008) estimates were assigned to each of the genes. The strict molecular clock model was used. A locus, which evolves fastest or is most divergent, was set as the reference locus to calibrate time and population (I used ADAMTS6 [a Z-linked intron] with a substitution rate of 1.6×10^{-9} substitutions/site/year and 15743 [showing high π values in both species; see Table 2.1] with a substitution rate of 1.35×10^{-9} substitutions/site/year in two separate analyses, respectively). The priors for parameters were adjusted according to preliminary runs. Each EBSP analysis included a MCMC chain of 500 million steps, sampled per 50,000 steps, and the first 25% of the steps were discarded as burn-in. Trace plots were checked using TRACER v 1.5 (Rambaut and Drummond 2007) to assess convergence in MCMC analyses and three independent runs were performed to assure convergence in estimates. If the 95% confidence interval (CI) of the estimate of the number of size-change steps exclude zero, I concluded there has been a significant population size change occurring (Lim and Sheldon 2011).

Test for neutrality of mtDNA using coalescence simulation

I tested departure from a neutral model in mtDNA using a neutral coalescent simulation program, SIMCOAL 2.1.2 (Laval and Excoffier 2004). The simulations were performed using the demographic parameters estimated from IMa and BEAST, i.e., current and ancestral effective population sizes, migration rates, divergence times, and scales and initial times of population expansion. The substitution rates of mtDNA, estimated based on nuclear-based divergence times and empirical nucleotide difference between the two

study species (see results), and the generation time of two years were used for the simulations. The ploidy of genes was taken into account for the simulations, i.e., the effective population size of mtDNA (N_{ef}) is $0.5 \times N_e$ of organisms assuming a balance sex ratio.

I simulated 10,000 data sets with the same sequence lengths and sample sizes as the empirical data for *F. parva* and F. *albicilla*. The simulated data sets were analyzed using Arlequin 3.1 (Schneider et al. 2000) to calculate π for each species. The π values of simulated data were compared with those of the empirical data to test whether the mtDNA genetic diversity of the two species departs from neutral expectations.

Test for positive selection on the mtDNA using likelihood ratio tests of hypotheses

ND2 sequences from another 15 *Ficedula* species and Cyt*b* sequences from another 17 *F.* sp. were downloaded from the NCBI GenBank (Supplementary table 2.2). Because these sequences were not all complete, the ND2 sequences were trimmed to 903 bp and the Cyt*b* sequences were trimmed to 975 bp to avoid alignment gaps. The CODEML program of the PAML 4.4 package (Yang 1997; Yang 2007) was used to detect positive selection in ND2 and Cyt*b* of *F. parva* and *F. albicilla*. Two unrooted phylogenetic trees of the genus *Ficedula*, one with 17 species for ND2 and one with 19 species for Cyt*b*, were modified from published studies (S□tre et al. 2001; Outlaw and Voelker 2006; Sangster et al. 2010) and used to estimate the ratio of nonsynonymous (replacement) to synonymous (silent) substitution rates ($\omega = dN/dS$) along the branches. The CODEML test assumes positive selection occur only when $\omega > 1$. Two branch-models were tested for the ND2 and Cyt*b* data. The null (one-ratio) model assumes all breaches have the same ω. The two-ratio model was used to estimate one ω (ω_a) for the branches leading to

F. parva and *albicilla* (I also specified ω_a for the branch leading only to *F. parva* or *F. albicilla* in two additional analyses) and another ω (ω_b) for the branches of all other *Ficedula* species. In addition, two site-models allowing ω vary among codons were used to detect particular sites under positive selection. The null M1a (nearly neutral) model assumes codons have either ω_0 or ω_1, as $0 < \omega_0 < 1$ and $\omega_1 = 1$; while the M2a (positive selection) model assumes there are the third type of codons with $\omega_2 > 1$. Finally, I used branch-site models which allow ω to vary among both branches and codons. The branch-site model A (we assigned it as BS-A in this study), combining the two-ratio and M2a models, are tested against a null model with ω_2 fixed at 1. Likelihood Ratio Tests (LRT) were used to test the three pairs of null and alternative models (i.e., one-ratio vs. two-ratio, M1a vs. M2a, and null vs. BS-A; see Yang et al. 2000). In addition, a sub-tree, only including the clade of *F. parva* and *F. albicilla* and its sister clade (totally four species for ND2 and six species for Cyt*b*; Supplementary table 2.2), was used to conduct the same model tests to compare with the results for the larger phylogeny, which may bring noise to the tests tending to focus on the two study species.

Modeling protein structure and locating amino acid replacement

The transmembrane (TM) and surface (SF) segments of membrane proteins can be under different selective pressure due to the structural and functional context (Wise et al. 1998; Tourasse and Li 2000). If natural selection affects evolution rate of mtDNA, replacement substitutions may tend to unequally distribute between TM and SF segments compared with silent substitutions.

The crystallized chicken Cyt*b* protein (3170C.pdb) and bovine heart COI protein (2occA.pdb) were used as templates to model three-dimensional structures for the two

proteins in *F. parva* and *F. albicilla* using the SWISS-MODEL online server (Schwede et al. 2003; Arnold et al. 2006; the online server at http://swissmodel.expasy.org/). I was unable to model the protein structure for ND2 of the study species because no proper crystallized structure was available as a template. The generated protein structures and the locations of amino acid replacement were visualized using the program Swiss-PdbViewer v4.02 (Guex & Peithsch 1997). The TM and SF segments in Cytb and COI proteins of these two flycatchers were predicted using MEMSAT (Jones et al. 1994) through the SWISS-MODEL server. The TM and SF segments in ND2 of the flycatchers were predicted using the program HMMTOP v2 (Tusnády and Simon 2001; the online server at http://www.enzim.hu/hmmtop/index.html) given the lack of a template for running analyses in the SWISS-MODEL server. I also used HMMTOP to predict the TM and SF segments for the Cyt*b* protein to compare the predictions from the two programs, MEMSAT and HMMTOP.

I tested whether the fixed replacement and silent substitutions between *F. parva* and *F. albicilla* tend to occur in either TM or SF segments of the mitochondrial proteins. I separated the substitutions between the two species into four categories, replacement TM, replacement SF, silent TM, and silent SF substitutions, to conduct Fisher's exact tests. This approach was similar to that of Wise et al. (1998) but overcame the problem of zero replacement and/or silent polymorphism in the mtDNA of the study species. This test took into account the difference in numbers of codons and constraint on nucleotide substitution between TM and SF segments. I applied this test to the ND2 and Cyt*b* (the Cyt*b* data lacked the first 39 codons) but not COI because I found only one fixed replacement substitution between the COI of the two species.

Results

Genetic diversity of mtDNA and nuclear DNA (ncDNA)

Cyt*b* sequences (1026 bp) were obtained for 16 *F. parva* (including one sample from Czech Republic downloaded from the GenBank) and 25 *F. albicilla* (NCBI accession numbers: *pending manuscript acceptance*); COI sequences (1551 bp) were obtained for 16 *F. parva* and 26 *F. albicilla* (NCBI accession numbers: *pending manuscript acceptance*; Table 2.1; see Supplementary table 2.3 for the geographic localities of the sequenced samples). The Cyt*b* sequences of one *F. parva* from Czech Republic and ND2 sequences of one *F. parva* from Sweden shared the same haplotypes with our own samples. MC1R sequences were obtained for 14 allele copies (two allele copies in one individual) in *F. parva* and 22 allele copies in *F. albicilla* (NCBI accession numbers: *pending manuscript acceptance*; Table 2.1; Supplementary table 2.3). Seventeen intron sequences were obtained for 13 to 24 allele copies for each species (mean = 18.5 for *F. parva* and 22.2 for *F. ablicilla*; NCBI accession numbers: *pending manuscript acceptance*; Table 2.1; Supplementary table 2.3). Most introns (15/17) contained one to six indels, which ranged from one to 61 bp (Table 2.1). There was no intra-locus recombination detected in these introns and exon.

There were three Cyt*b* haplotypes in *F. albicilla*, but two of them differed only by one bp from the common haplotype and were possessed by single individuals. There was one singleton, other than the dominant one, in the COI sequences of *F. albicilla*. Pi (π) was consistently lower for *F. albicilla* (0.00007 ± 0.00005 [SE]) than for *F. parva* (0.00141 ± 0.00029) in all three mtDNA regions, although π for *F. albicilla* was not zero

for Cyt*b* and COI as was for ND2 (Table 2.1; Fig. 2.2). In contrast, π for the nuclear loci were not significantly different between the two species (0.00536 ± 0.00116 for *F. albicilla*. and 0.00546 ± 0.00086 for *F. parva* at introns, $p = 0.936$, paired Student's t-test; 0.00164 for *F. albicilla*. and 0.0027 for *F. parva* at MC1R; Fig. 2.2). Two introns had no genetic variation among the samples of one species (i.e., 00132 in *F. albicilla* and ABCA1 in *F. parva*; Table 2.1). No intra-locus recombination was detected in the 18 nuclear loci.

Neutrality tests

For the datasets containing all individuals of both species, the HKA tests could not reject the neutral model for the 17 introns plus one exon, the 17 introns, and the 15 introns excluding 00132 and ABCA1 ($p = 0.28$, 0.21, and 0.42). However, the HKA tests always rejected the neutral model for the datasets in which any of the ND2, Cyt*b*, and COI data were added ($p = 0.002 – 0.038$). The same conditions applied to the datasets containing all *F. albicilla* and one *F. parva*, but not to those containing all *F. parva* and one *F. albicilla*, in which adding mtDNA did not change the insignificant results. These results suggested that mtDNA variation of *F. albicilla* but not *F. parva* departed from the neutral expectation.

Demographic and divergence history

The IMa analyses based on the 17 introns suggested similar effective population sizes for *F. parva* (654,876, 95% CI = 524,777 – 837,710) and *F. albicilla* (754,922, 95% CI = 610,042 – 952,169; Table 2.2). The effective population size of their common ancestor (663,658, 95% CI = 389,416 – 1,259,636) was similar to those of the two species, although its CI was larger than those of the two species. The divergence time between

these two species was 3,112,058 (95% CI = 2,492,660 – 4,169,719) years ago. There was no gene flow between the two species since divergence (Table 2.2). The analyses based on the 17 introns plus one exon or the 15 introns suggested similar histories as those based on the 17 introns (Table 2.2).

The EBSP analyses showed that *F. albicilla* has experienced recent population expansion whereas *F. parva* has had a stable effective population size (Fig. 2.3; the 95% CIs of the estimated number of size-change steps were 1 - 2 for the former and 0 - 1 for the latter). These results seemed to conflict with the IMa estimates, which showed that both species have similar effective population sizes relative to their common ancestor (Table 2.2). EBSP is thought by some to provide a better picture of complex demographic scenarios than IMa (Rovito 2010). However, the absolute population sizes and initial times of population expansion estimated by EBSP depended on the choice of a reference locus and its substitution rate. For example, the current effective population sizes of *F. albicilla* were 23,500 (Fig. 2.3) and 867,000 when ADAMTS6 and 15743 were used as the reference loci, respectively. The initial time of *F. albicilla* population increase was around 12,000 (Fig. 2.3) and 390,000 years ago when ADAMTS6 and 15743 were the reference loc, respectively. Nevertheless, the scale of population increase (~ 6 times larger) and the ratio of current population size to initial time of population expansion (~ 2) were consistent across different reference loci. I considered the absolute estimates of current population sizes from IMa to be more reliable given it was based on the geometrical mean of the substitution rates of all the loci. Thus, I combined the IMa and EBSP estimates to obtain a better picture of demographic history for these two species (scaled for mtDNA in Fig. 2.4a, which was based on the 15 introns excluding

00132 and ABCA1). The result based on the 17 introns was that the two species diverged from each other around 3.1 million years ago when the ancestral population size was around 650,000, *F. parva* has remained at a similar and constant population size since then, and *F. albicilla* has experienced recent population increase (~ 6 times larger) around 390,000 years ago to the current population size of 750,000. I assumed a bottleneck in *F. albicilla* when it split from *F. parva* (Fig. 2.4a) and this was more conservative for testing against a neutral pattern (using coalescence simulation) than assuming no bottleneck. In other words, if the null hypothesis (a neutral pattern) is rejected, we can conclude that there was factor(s) other than a bottleneck driving the observed low mtDNA polymorphism of *F. albicilla*. I acknowledge that there was uncertainty in the estimates of divergence times and population sizes. Therefore, I also used values 2.5 times smaller and larger than the above estimates (over the range of 95% highest posterior density [HPD] of EBSP estimates, Fig. 2.3) to conduct additional simulations, and the conclusions did not change. Hence, only the results of the first setting were reported.

Test for neutral pattern of mtDNA using coalescence simulation

The demographic scenario based on the IMa and EBSP analyses was used to simulate a neutral pattern of mtDNA nucleotide diversity (Fig. 2.4a). The IMa inferences based on the 15 introns, instead of all the17 introns, were used considering the potentially non-neutral pattern of the two introns, 00132 and ABCA1 (although the IMa results of the two data sets were similar). Because the nucleotide difference between the two species were 0.06854, 0.06069, and 0.05027 in ND2, Cyt*b*, and COI (Table 2.1) and the divergence time was about 3.327 million years (based on the 15 introns; Table 2.2), I calculated the

substitution rates for the three mtDNA regions as 0.0103, 0.0091, and 0.0076 per site per million years, respectively.

The comparison of the simulated and empirical data rejected a neutral pattern for the mtDNA of both *F. parva* and *F. albicilla*. The π values of both species in ND2 were out of the range of π values for the simulated neutral data, which took into account the population size change (Fig 4b). The same conclusion was applied to the Cyt*b* and COI data of the two species (data not shown).

Test for positive selection in the mtDNA using likelihood ratio tests of hypotheses

For the branch-model test in ND2, the log-likelihood value (ℓ_0) under the one-ratio model was -5126.5 with $\omega = 0.047$ and the log-likelihood value (ℓ_1) under the two-ratio model was -5126.46 with $\omega_a = 0.042$ and $\omega_b = 0.047$. The LRT could not reject the one-ratio model; $2\Delta\ell = 2(\ell_1 - \ell_0) = 0.08$ with the χ^2 distribution (df = 1) has $p = 0.78$ (Table 2.3). Two additional tests, which assigned ω_a to the branch leading only to *F. parva* or *F. albicilla*, showed similar results ($p = 0.56$ and 0.62). The tests based on cyt*b* showed similar results ($p = 0.25$, Table 2.3; $p = 0.84$ and 0.15 for the two additional tests assigning ω_a to the branch leading only to *F. parva* or *F. albicilla*).

For site-model test in ND2, the ℓ_0 under the M1a model was -5054.7 suggesting 94.8% of sites with $\omega_0 = 0.027$ and 5.2% of sites with $\omega_1 = 1$. The ℓ_1 under the M2a model was the same as ℓ_0 and suggested 0% of sites with $\omega_2 > 1$ (Table 2.3). Given $2\Delta\ell = 0$ ($p = 1$), there was no evidence for positive selection on the ND2 data. The test based on Cyt*b* showed the same result (Table 2.3). The branch-site models returned almost the same results as the site model tests for both ND2 and Cyt*b* (Table 2.3).

The results based on a sub-tree with reduced species numbers suggested the same conclusion of no evidence for positive selection in the ND2 and Cyt*b* data, although they tended to return slightly lower *p*-values than those based on the whole trees (Table 2.3).

Amino acid replacements in TM and SF segments

Replacement substitutions tended to occur in the TM regions (12 TM : 1 SF) of the ND2 protein more than silent ones (30 TM : 24 SF; $P_{\text{one-tail}} = 0.012$, Fisher's exact test; Table 2.4). I also found more TM replacement substitutions (n = 8) in the Cyt*b* protein (one SF replacement substitution; Fig. 2.5; Table 2.4), although the ratio of TM and SF was not significantly different between the replacement and silent substitutions ($P_{\text{one-tail}} = 0.083$, Fisher's exact test; Table 2.4). The TM predictions of the Cyt*b* protein made by MEMSAT and HMMTOP were very similar, and the results of Fisher's exact test based on the two predictions were the same. Thus, I consider the TM prediction of ND2 based on HMMTOP to be reliable.

Discussion

This study shows that although *F. albicilla* experienced a recent population expansion perhaps following a historical population bottleneck, this demographic history cannot fully explain the extremely low genetic diversity in its mtDNA. In fact, the polymorphism of mtDNA in both *F. albicilla* and *F. parva* departs from the neutral expectation based on coalescence simulation. These results imply that their mtDNA genomes are subject to positive selection or linked to other genes under positive selection (selective sweeps; Maynard-Smith and Haigh, 1974). I address the striking mtDNA pattern of these two flycatchers from different perspectives.

Contrasting genetic diversity between mtDNA and ncDNA

The polymorphism of mtDNA in *F. albicilla* was consistently smaller than that of *F. parva* across the three regions, ND2, Cyt*b* and COI. Therefore, it is highly unlikely that the lack of polymorphism in ND2 of *F. albicilla* is an artifact of sequencing a pseudogene because nuclear copies should not occur in all three regions that together span half of the avian mtDNA genome (Pereira and Baker 2004b). Furthermore, I observed that (1) the PCR for ND2 based on four different pairs of primers (including one pair for amplifying half of the mtDNA genome and another for about 4,000 bp) returned the same results, (2) there were no indels or extra stop codons found, (3) correct sister relationship between the two species and between their clade and the other clade were obtained based on the ND2 data (results not shown), and (4) the estimated substitution rate of ND2 (0.0103 per site per million years) was close to those of other avian species (Arbogast et al. 2006, Lovette 2004, Wier and Schluter 2008), supporting the validation of the ND2 data (Calvignac et al. 2011).

The polymorphism of ncDNA and the estimated N_e using IMa based on multiple ncDNA were not significantly different between *F. albicilla* and *F. parva*. Therefore, differences in current N_e cannot explain the low level of polymorphism in *F. albicilla*. However, the EBSP revealed a recent population expansion in *F. albicilla* but not *F. parva*. Thus, historical population changes need to be taken into account when assessing the effect of demographic factors in the mtDNA patterns of the two flycatchers.

Another conspicuous pattern found is that the polymorphism of mtDNA was smaller than ncDNA in both species (Fig. 2.2; Table 2.1), whereas the divergence between the two species was larger in mtDNA (0.05983 ± 0.00529 [SE]) than ncDNA

(0.01307 ± 0.00119 for introns and 0.00581 for MC1R; Table 2.1). Given that the N_e of mtDNA is one-fourth that of ncDNA and the substitution rate of mtDNA is larger than that of ncDNA (Arbogast et al. 2006; Ellegren 2007; Wier and Schluter 2008), the contrasting intra- and inter-specific patterns between mtDNA and ncDNA of the two flycatchers could be merely one realization of the stochastic (neutral) coalescence processes. Thus, the following coalescence-based analyses are applied to examine these striking patterns.

Departure from the neutral pattern at mtDNA of the two flycatchers

I used neutral coalescence simulation which assumes a historical population bottleneck and a recent population expansion in *F. albicilla* but not *F. parva* to test (1) whether the different demographic histories can explain the different mtDNA diversity between the two flycatchers and (2) whether the stochastic coalescence processes and difference in N_e and substation rates can explain the contrasting pattern between their mtDNA and ncDNA. The simulation results predicted only slightly lower polymorphism in *F. albicilla* than in *F. parva* (Fig. 2.4b). Thus, different demographic histories cannot fully explain the extremely low mtDNA polymorphism in *F. albicilla*, which departs from the neutral expectation based on the simulation (Fig. 2.4b). Surprisingly, the observed mtDNA polymorphism of *F. parva* is also significantly lower than the neutral expectation (Fig. 2.4b). In fact, the mtDNA polymorphism of *F. parva* (π_S [silent nucleotide polymorphism] = 0.0047 ± 0.0006 [SE], π_N [replacement nucleotide polymorphism] = 0.0003 ± 0.0002) is lower than other avian species (π_S = 0.02 – 0.06, π_N = 0.0015 - 0.005 for 72 avian species, see Hughes and Hughes 2007). Of course, the mtDNA polymorphism of *F. albicilla* is even much lower than other avian species. It also

suggests that the mtDNA variation patterns of the two flycatchers might be atypical in birds and should not be used as a general condemnation of the application of mtDNA in phylogeography.

The HKA tests suggested a departure from neutral expectation for the mtDNA of *F. albicilla*, but less likely for *F. parva*. In other words, selection-related forces are likely responsible for the low polymorphism of the mtDNA of the two species, particularly *F. albicilla*.

Test for positive selection targeting on mtDNA of the two species

The CODEML tests suggest no evidence for positive selection in either ND2 or Cyt*b* of these two species. The CODEML test assumes positive selection occurs only when dN/dS > 1, i.e., repeated replacement substitutions in a single codon or numerous replacement substitutions accumulate in a particular lineage (Yang and Bielawski 2000). However, it has been shown that one or a few replacement substitutions can result in adaptive phenotypic changes (e.g., Hoekstra et al. 2006). If true, this test as well as other similar statistic methods for detecting positive selection can be fatally biased (Yang and Bielawski 2000; Hughes 2007). Therefore, the insignificant results cannot rule out the possibility that positive selection targeting on the mtDNA of these two flycatchers.

The distribution of amino acid replacements in TM and SF segments

The TM segments accumulate more replacement substitutions than the SF segments when comparing the mtDNA, especially ND2, of the two flycatchers, which is different from some studies. To explore the unique pattern found between the two study species, I applied the same test to the ND2 sequences of 28 *F. hyperythra* versus two *F. westermanni*. The results showed that there was not significantly more replacement

substitutions in the TM than in SF segments ($P_{\text{one-tail}}$= 0.209, Fisher's exact test; data not shown). Kerr (2011) found replacement substitutions equally distributed between helix (primarily TM) and loop (primarily SF) sites based on COI data from 43 avian species across 12 orders. Kerr (2011) also suggested that there is no evidence for a selective sweep in the avian COI. Tourasse and Li (2000) reported that the TM segments accumulate fewer replacement substitutions than the SF segments of proteins in mammals across six orders. They suggested that negative selection limits substitutions in TM segments, which therefore are subject to more stringent structural constraint. The contrasting patterns between this and other studies imply that the ND2 protein of either *F. parva* or *F. albicilla* or both can be under positive selection, or at least depart from neutral expectation. In addition, I found that six of the eight replacement amino acid residues in the Cyt*b* TM form three pairs, in which the residues were physically close to each other (the distances between residue α carbon were 5.9 to 6.2 Å; Fig. 2.5). The clusters of replacement substitutions could reflect the influence of positive selection (Castoe et al. 2008). However, a strong inference of positive selection on the mtDNA of *F. albicilla* and *F. parva* cannot be drawn in this study and require further studies on phenotypic changes linked to the replacement substitutions (Ballard and Melvin 2010) or functional test for mitochondrial-nuclear co-adaptation (Tieleman et al. 2009).

Alternative explanations for low mtDNA variation

Even if the examined regions of mtDNA (i.e., ND2, Cyt*b* and COI) are not directly subject to positive selection, (1) linkage to other selected regions or genes or (2) mitochondrial-nuclear co-adaptation can also lead to low genetic variation in these mtDNA regions. If a favorable allele becomes fixed in any region of mtDNA, the lack of

recombination in mtDNA can lead to fixation of neutral or mildly deleterious alleles in other regions (Oliveira et al. 2007). In addition, because mtDNA and W chromosome are both maternally transmitted (i.e., have the same segregation process and thus are linked) in birds, the genetic polymorphism of mtDNA could be reduced if genes on the W chromosome are under strong positive selection (Berlin et al. 2007). Furthermore, because of the co-adaptation between nuclear and mitochondrial genes, which encode cooperated peptides for cellular energy production, the variation of mtDNA could be influenced by selective enforces targeted on mitochondrion-associated ncDNA (Gershnoi et al. 2009). If the low mtDNA variation of the two flycatchers is caused by indirect selective forces through hitchhiking (Maynard-Smith and Haigh 1974) or co-evolution, we cannot find the sites under selection by only examining these three mtDNA regions. However, even though scanning a whole genome is possible now, testing positive selection for every candidate gene in detail is still a formidable job.

Confounding effect of demographic history and selective force in genetic signature

The nuclear-based demographic history was incorporated into coalescence simulation to test if the mtDNA of the flycatchers departs from the neutral expectation in this study. I acknowledge that the estimated history can be over-simplified and a more complex and dynamic history (e.g., repeated bottleneck and expansion) can probably change the conclusion to neutral mtDNA in the study species. However, such uncertain situations should only apply to the mtDNA of *F. parva* but not *F. albicilla* because the genetic polymorphism of the former is smaller than an average of other birds by a factor of 10, whereas for the latter is a factor of 100 or more.

I suggest that neither positive selection nor population bottleneck alone result in the strikingly low variation of *F. albicilla* mtDNA. It is more likely that demographic and selective forces act in concert to contribute to the pattern that one, and only one, ND2 haplotype is shared by 75 individuals sampled from a range spanning over 4,500 kilometers (Zink et al. 2008). During a population bottleneck, genetic drift reduces genetic variation and increases the frequencies of initial rare (neutral or advantageous) alleles; during the following population expansion, positive selection or genetic draft can dramatically increase the fixation rate of advantageous mutations or their linked mutations (Gillespie 2001; Meiklejohn et al. 2007). Thus, if population bottleneck and expansion occur repeatedly in the history of *F. albicilla* and its mtDNA are subject to positive selection either directly or indirectly, we can expect the fixation of an allele even in a currently large population.

Table 2.1. Characteristics of the 19 genes (the three mtDNA regions belong to the same gene) in this study. Chr indicates the chromosome where the gene is located. L indicates the length of the gene used in the analyses. N_{FIPA} and N_{FIAL} show the sample size (in numbers of alleles) of *Ficedula parva* and *F. albicilla*, respectively in each gene. π indicates the nucleotide diversity of each species. Dxy indicates the nucleotide divergence between the two species. Indel length shows the length of individual indel in the corresponding gene.

Gene	Chr	L	N_{FIPA}	N_{FIAL}	π_{FIPA}	π_{FIAL}	Dxy	Indel length
ND2	Mt[a]	1041	17	75	0.00138	0	0.06854	
Cyt*b*	Mt[a]	1026	16	25	0.00193	0.00016	0.06069	
COI	Mt[a]	1551	16	26	0.00092	0.00005	0.05027	
				Mean	0.00141	0.00007	0.05983	
00132	26	324	20	24	0.00332	0	0.00549	6
06635	6	540	20	24	0.00541	0.00749	0.01767	2, 4, 5
08352	5	348	20	24	0.00166	0.00378	0.01468	1
09385	20	283	20	22	0.00802	0.01859	0.01397	1, 1, 4, 7, 7, 7
11074	20	376	18	22	0.00688	0.00656	0.01013	15
12021	24	633	20	24	0.00125	0.00026	0.00891	1
13380	7	686	20	24	0.00814	0.00159	0.01882	1, 1, 1
14765	3	817	20	24	0.00462	0.00565	0.01245	1, 1
15743	1	530	16	24	0.01372	0.00931	0.02686	1, 10, 10
17483	4	491	20	24	0.00412	0.00750	0.01211	1, 5
ACL	27	372	16	24	0.00690	0.00657	0.01384	1
AK	17	707	18	24	0.00960	0.00602	0.01231	2, 61, 61, 61
MPP	4	216	18	22	0.00732	0.00459	0.00657	1
RHO	12	779	16	22	0.00090	0.00023	0.01214	1
TGFB2-I5	3	518	18	24	0.00703	0.00032	0.01099	
ABCA1	Z	281	17	13	0	0.01058	0.01122	
ADAMTS6	Z	529	17	13	0.00390	0.00210	0.01408	1, 1
				Mean	0.00546	0.00536	0.01307	
MC1R	11	590	14	22	0.0027	0.00164	0.00581	

[a] mitochondrial DNA

Table 2.2. Coalescence analyses using IMa. Current effective population sizes of *Ficedula albicilla*, *F. parva*, and their common ancestor are denoted by $N_{e(FIAL)}$, $N_{e(FIPA)}$ and $N_{e(anc)}$, respectively. m_1 indicates the number of individual per generation migrating from *F. parva* to *F. albicilla* and m_2 indicates the migration in the other direction. t indicates the divergence time between *F. parva* and *F. albicilla* in the unit of years. These analyses are based on 15 introns, 17 introns, and 17 introns plus one exon, respectively. HiSmth indicates the value of the highest posterior probability after been smoothed using surrounding points. 95Lo indicates the value to which 2.5 % of the total distribution lies to the left. 95Hi indicates the value to which 2.5 % of the total distribution lies to the right.

		$N_{e(FIAL)}$	$N_{e(FIPA)}$	$N_{e(anc)}$	m_1	m_2	t
15 introns	HiSmth	820,666	742,987	749,649	0	0	3,327,422
	95Lo	662,270	594,115	451,984	0	0	2,645,477
	95Hi	1,039,143	954,096	1,467,906	0.0399	0.0372	4,432,643
17 introns	HiSmth	754,922	654,876	663,658	0	0	3,112,058
	95Lo	610,042	524,777	389,416	0	0	2,492,660
	95Hi	952,169	837,710	1,259,636	0.0354	0.0330	4,169,719
17 introns	HiSmth	758,884	660,159	653,003	0	0	3,229,241
+ 1 exon	95Lo	616,531	531,170	375,327	0	0	2,569,250
	95Hi	951,031	841,109	1,215,532	0.0334	0.0306	4,232,697

Table 2.3. Likelihood ratio statistics of model test for positive selection in ND2 and Cyt*b* using CODEML program in PAML 4.4. Branch model test is conducted by comparing one-ratio and two-ratio models. Site model test is conducted by comparing M1a (nearly neutral model) and M2a (positive selection model). Branch-site model is conducted by comparing BS-A (combined two-ratio and M2a model) and the corresponding null model. $2\Delta\ell$ indicates twice the log likelihood difference between the two compared models. df indicates the degree of freedom and *p* indicate the *p* value from χ_1^2. The numbers in the parentheses were results based on a sub-tree with four species for ND2 or six species for Cyt*b*.

	Comparison of Models	$2\Delta\ell$	df	*p*
ND2	One-ratio vs. Two-ratio	0.08 (0.52)	1	0.78 (0.65)
	M1a vs. M2a	0 (0)	1	1.00 (1.00)
	null vs. BS-A	0 (0.13)	1	1.00 (0.72)
Cyt*b*	One-ratio vs. Two-ratio	1.34 (1.72)	1	0.25 (0.19)
	M1a vs. M2a	0 (4.38)	1	1.00 (0.11)
	null vs. BS-A	0 (0)	1	1.00 (1.00)

Table 2.4. Numbers of fixed replacement and silent substitutions between *Ficedula parva* and *F. albicilla* at the transmembrane and surface segments of ND2 and Cyt*b* regions. FET probability indicates the probability of Fisher's exact one-tail test.

	ND2		cyt*b*	
Fixed substitution	Transmembrane	Surface	Transmembrane	Surface
Replacement	12	1	8	1
Silent	30	24	30	21
FET probability:	0.012		0.083	

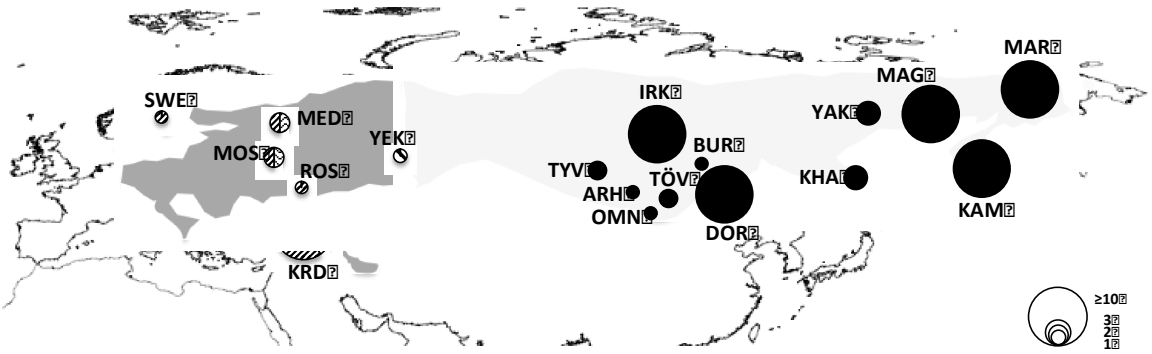

Figure 2.1. Breeding ranges of *Ficedula parva* (dark gray patch) and *F. albicilla* (light gray patch) and distribution of mtDNA ND2 haplotypes. Colors (or patterns) of circle indicate haplotypes. Sizes of circle proportion to numbers of individuals sampled in the location. ARH indicates Arhangay, BUR indicates Buryatiya, DOR indicates Dornod, IRK indicates Irkutskaya, KAM indicates Kamchatka, KHA indicates Khabarov, KRD indicates Krasnodar, MAG indicates Magadan, MAR indicates Markovo, MED, Medvedevo, MOS indicates Moscow, OMN indicates Omnogovi, ROS indicates Rostov, SWE indicates Sweden, TYV indicates Tyva, TÖV indicates Töv, YAK indicates Yakutiya and YEK indicates Yekaterinburg.

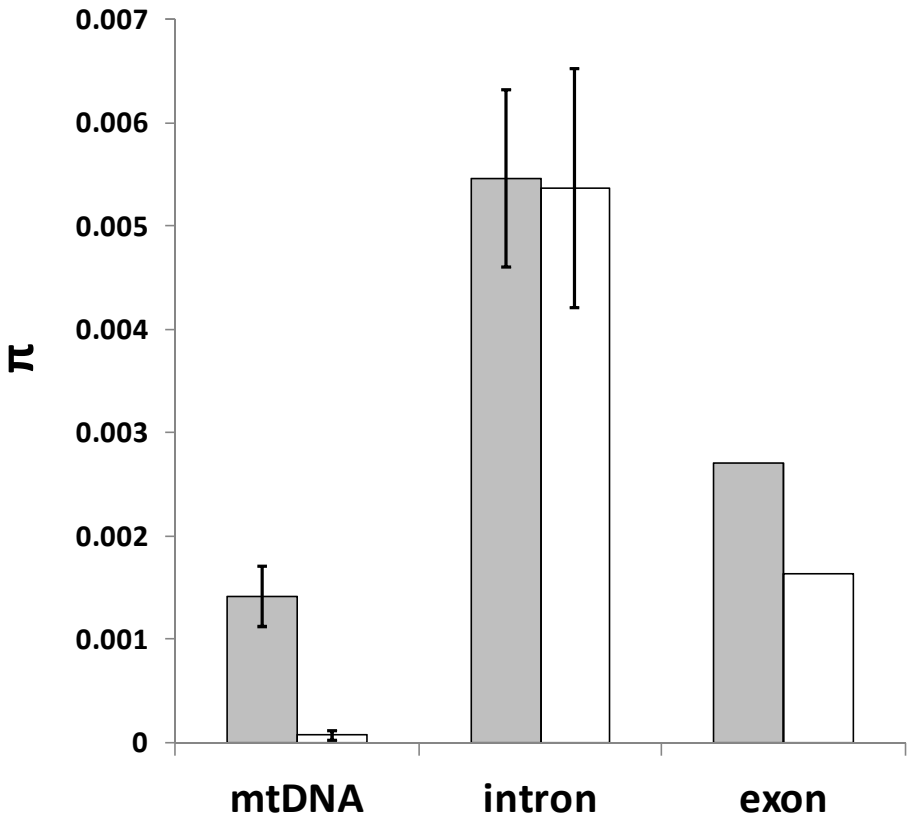

Figure 2.2. Nucleotide diversity (π) of three mtDNA regions, 17 introns, and one exon of *Ficedula parva* (gray bars) and *F. albicilla* (white bars). Shown are means and standard errors for mtDNA and introns.

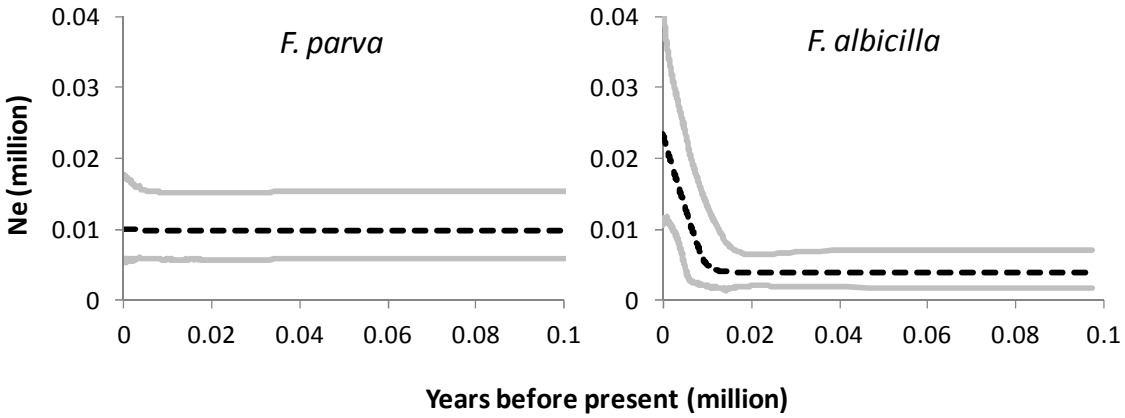

Figure 2.3. Extended Bayesian Skyline Plots of population sizes of the two study species. Black dashed lines indicate median values. Grey lines indicate 95% highest posterior density (HPD). ADAMTS6 is set as the reference locus to calibrate time and population in this figure.

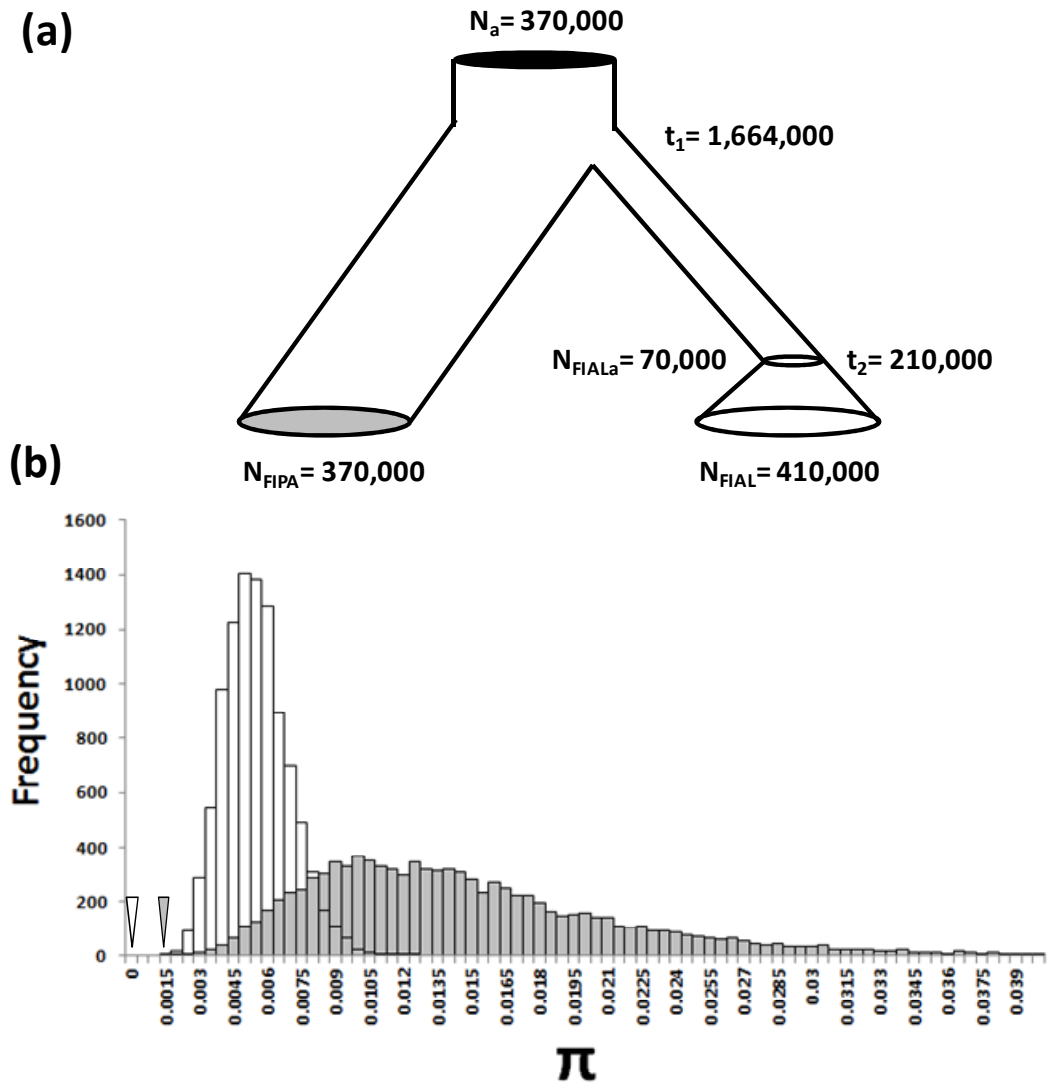

Figure 2.4. (a) Outline of the demographic model based on IMa and EBSP estimates (based on the 15 introns exclduing 00132 and ABCA1) used to simulate neutral mtDNA seqeuces of the two study species. N_a, N_{FIPA}, N_{FIAL}, and N_{FIALa} indicate effecive population sizes of mtDNA for the common ancestor of the two study speceis, *Ficedual parva*, *F. albicilla*, and the latter before recent population expansion, respectively. t_1 and t_2 indicate time of divergnce between the two species and population expanion of *F. albicilla* in units of generations from present, respectively. (b) Distributions of nucleotide diversity (π) values for 10,000 neutrally simulated ND2 data sets for each of *F. parva* (grey bars) and *F. albicilla* (white bars). The grey triangle represents the empirical π value of ND2 in *F. parva* and the white one for *F. albicilla*.

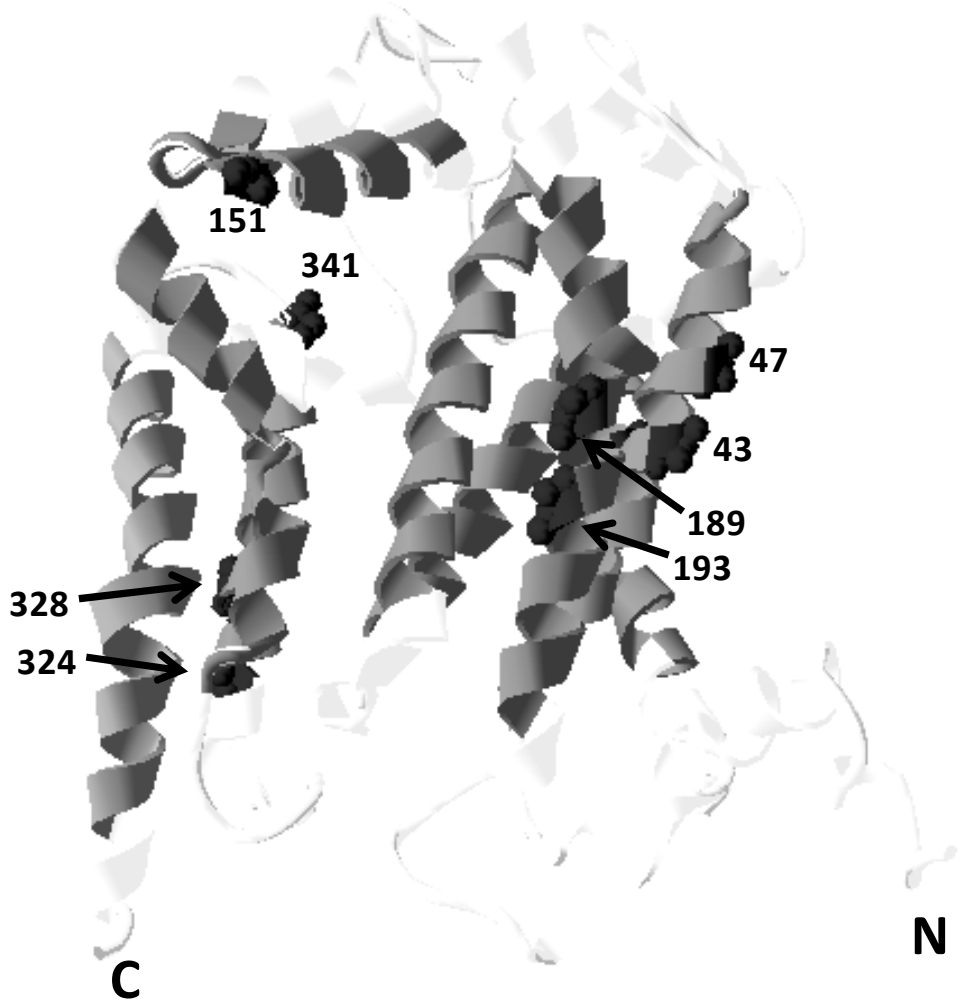

Figure 2.5. Three-dimensional (3D) representation of fixed amino acid replacements between *Ficedual parva* and *F. albicilla* in the Cyt*b* protein. The location of replacement amino acid residue is emphasized using black 3D structure of atoms and the codon order number (One replacement codon, the 241st codon, cannot be seen in this side). Dark grey color indicates transmembrane segments and white color for surface segments. N and C indicate N- and C-terminus of the Cyt*b* protein. Three pairs of replacement amino acid residues in the transmembrane (i.e., the 43rd and 47th, the 189th and 193rd, and the 324th and 328th) were physically close to each other (the distances between residue α carbon were 5.9 to 6.2 Å).

Chapter 3

Recent allopatric divergence and niche evolution in a widespread Palearctic bird, the common rosefinch (*Carpodacus erythrinus*)

Hung, C.-M., S. V. Drovetski, and R. M. Zink. (submitted to *Molecular Phylogenetics and Evolution*)

Phylogeographic analysis of the widespread common rosefinch (*Carpodacus erythrinus*) revealed three recently diverged groups, corresponding to the Caucasus, central-western Eurasia, and northeastern Eurasia. The mtDNA gene tree showed that a majority of haplotypes from the Caucasus were related, whereas the other two groups were not distinguished. By contrast, UPGMA clustering of mtDNA Φ_{ST}-values among populations recovered the three groups. A sex-linked gene tree recovered no phylogeographic signal, which we attribute to recent divergence and insufficient time for sorting of alleles. Coalescence methods corroborated the existence of three groups of populations, revealing a lack of gene flow, and population expansion in the two northern groups, the central-western and northeastern Eurasia. These three groups correspond to named subspecies, further supporting their validity. A species distribution model revealed potential allopatric Last Glacial Maximum refugia. These three groups, which appear to be at the early stage of speciation, provide a good opportunity for testing ecological speciation. Ecological niche tests showed that ecological divergence has not been prevalent in the early stages of speciation of these three taxa.

Introduction

Quaternary climatic fluctuations repeatedly shifted the distributions of species, presumably resulting in multiple cycles of retraction into refugia during glaciation and subsequent expansion during interglacial periods (Hewitt, 2000; 2004). These fluctuations in range could have had at least three consequences: 1) initiation of divergence among populations, 2) continued maintenance of already distinct populations, or 3) merging of once-differentiated populations. Phylogeographic studies can provide a description of the current geographic deployment of genetic variation and provide inferences about recent evolutionary history (Avise, 2000). For example, the discovery of three phylogroups in an extant species implies the existence of at least three allopatric glacial refugia at the Last Glacial Maximum (LGM; 21,000 years ago), assuming that the groups evolved during or prior to the last glacial period. One could construct a species distribution model (SDM), often referred to as a niche model (Peterson et al., 1999), to determine the sizes and locations of LGM refugia and then relate them to the current population structure (Carnaval et al., 2009; Knowles and Alvarado-Serrano, 2010). One could also discover whether these groups have diverged ecologically, providing a potential test of the tenets of ecological speciation (Schluter, 2009, McCormack et al., 2010). Because ecological divergences could occur after speciation, comparison of those that are very recently diverged enhances tests of niche divergence. Therefore, combining phylogeographic analysis with SDMs provides a more in-depth picture of species' recent histories than either source of information can by itself.

In this study, we evaluate ecological divergence among three recently isolated groups of a widespread Palearctic bird, the common rosefinch (*Carpodacus erythrinus*).

The common rosefinch inhabits various types of woodlands and grasslands, spanning much of the Palearctic. During the past century, its range has expanded westward into Scandinavia, France, Spain and England (Cramp and Perrins, 1994; Payevsky, 2008), although persistent breeding is limited to Scandinavia. Pavlova et al. (2005) surveyed mtDNA variation and postulated the existence of three incompletely isolated groups corresponding to the Caucasus (CA), northeastern Eurasia (NEE), and central-western Eurasia (CWE, Fig. 3.1). However, the geographic limits of the groups were unclear and maximum likelihood estimates of migration suggested a low level of gene flow among these groups. In this study, we (1) re-examined the conclusion of Pavlova et al. (2005) using robust coalescence methods and adding a Z-linked gene, (2) used a SDM to reconstruct the current and LGM distributions of the common rosefinch, to search for sites of potential refugia, and to assess the relative sizes of populations at each time, and (3) tested for ecological divergence between these groups to determine if niche differentiation has accompanied the early stages of lineage divergence (Warren et al., 2008).

Methods and Materials

Genetic analyses

We used the ND2 sequence data for 186 common rosefinches from Pavlova et al.'s (2005) study (Fig. 3.1, NCBI accession numbers AY703261-AY703446). In addition, one Z-linked intron, ADAMTS6 (Backström et al., 2006), was sequenced for samples from 14 localities (11, 7, and 10 individuals from the three mtDNA-defined groups, respectively). Phases of sequences containing indels were sorted manually by subtracting

chromatogram peaks upstream of the indel in the reverse primer sequences from the double peaks downstream of the indel in the forward primer sequences. This was repeated in the alternative direction and allowed the two alleles of a heterozygous individual to be determined (Sousa-Santos et al., 2005; Dolman and Moritz, 2006). Alleles present in individuals with multiple heterozygous sites but no indel(s) were resolved using PHASE 2.1.1 (Stephens et al., 2001; Stephens and Scheet, 2005).

Detection of population division

NETWORK 4.5.1.6 (fluxus-engineering.com) was used to generate minimum spanning networks (Polzin and Daneschmand, 2003) for mtDNA and ADAMTS6 data to detect geographic partitioning of haplotypes and alleles. In addition, pairwise Φ_{ST}-values of mtDNA (but not ADMATS6 due to small sample sizes) among populations were estimated using DnaSP 5 (Librado and Rozas, 2009). To determine the overall geographic pattern of population structure, we pooled individuals from each locality and then clustered the matrix of pairwise Φ_{ST} values using the unweighted pair-group method using arithmetic averages (UPGMA) implemented in MEGA 4 (Tamura et al., 2007). We combined the localities with sample sizes smaller than five with samples in other nearby localities to avoid bias in Φ_{ST} estimates. If the combination was not geographically reasonable, the small populations were excluded from analyses. For example, the Sakhalin population was not combined with the Kamchatka or Magadan population because they are separated from each other by a wide area of sea or a large long geographic distance.

Estimates of demographic parameters

A coalescence-based program, IMa (Hey and Nielsen, 2007), was used to estimate the effective population sizes of two current and their common ancestral populations (θ_1, θ_2, and θ_a; $\theta = 4N_e\mu$), migration rates (m_1 and m_2; $m = m/\mu$), and divergence times ($t = t\mu$) between groups of populations determined from the procedures outlined above. We did not use IMa2 (Hey, 2010) because we cannot specify a tree topology for the three groups. A minimum of two independent analyses of $> 2\times10^7$ steps after a burn-in of 10^6 steps were performed for each pairwise comparison. Plots of trend lines and the effective sample size values (ESS > 250) were examined to assess convergence in parameter estimates. The IMa estimates were based on the mtDNA and AMADTS6 data combined. To convert the scaled demographic parameters to absolute values, we calculated the geometric mean of the substitution rates of ND2 and ADAMTS6 by multiplying the sequence lengths by 4×10^{-8} substitutions/site/year for ND2 (Arbogast et al., 2006) and 1.62×10^{-9} substitutions/site/year for ADAMTS6 (Ellegren, 2007; given the mean divergence of Z-linked introns between chicken and turkey is 1.2 times higher than that of autosomal introns, which have an average rate of 1.35×10^{-9} substitutions/site/year) and assumed the generation time is two years (Stjenberg 1979). The substitution rate used in this study was higher than widely used rates for avian mtDNA (Lovette, 2004; Weir and Schluter, 2008) but more appropriate for recent divergences (Arbogast et al., 2006; Herman and Searle, 2011).

Group delimitation using simulation and hypothesis testing

We tested alternative population models using a coalescent simulation program, SIMCOAL 2.1.2 (Laval and Excoffier, 2004) to simulate ND2 sequences. The simulations were performed using the demographic parameters estimated from IMa based on mtDNA and ADAMTS6, i.e., current effective population sizes (the effective population size of mtDNA, N_{ef}, was assumed as to be half of the N_e of populations), migration rates, divergence times, exponential growth rates (calculated from the current and ancestral population sizes), a substitution rate of 4×10^{-8} substitutions/site/year, and the generation time of two years.

We simulated 5,000 data sets of 186 ND2 sequences (1041 bp) for each hypothesized model (described in results). The simulated data sets were analyzed using Arlequin 3.1 (Schneider et al., 2000) to calculate Φ_{ST} values (Excoffier et al., 1992) and the distribution and the upper and lower bounds of 95% ranges of these values were recorded. The Φ_{ST} values of simulated data were compared with the Φ_{ST} of the empirical data to evaluate which model was most consistent with the observed data.

Species distribution modeling

Online databases ORNIS and GBFI together with our own museum data resulted in 196 breeding localities which we input into MAXENT v 3.2.2. (Phillips et al., 2006) to infer a SDM. Because the species has only recently colonized western Europe, we excluded breeding records from France, Spain and England. We obtained climatic data (19 layers) for present and LGM conditions from the Worldclim bioclimatic database (Hijmans et al., 2005), and we ran MAXENT using 30% of values for training, and constructed a SDM

from the average of 10 MAXENT runs that we displayed using DIVA-GIS ver. 7.1.7.2 (Hijmans et al., 2004).

Niche divergence tests

We used the program ENMTools v1.3 (Warren et al., 2010) to perform niche identity tests and background tests for whether taxa (which were defined according to the genetic data, i.e., the CA, CWE and NEE groups) exhibit niche divergence or conservatism (or neither). The niche identity test assesses whether the similarity between ecological niches of two taxa (measured by the niche similarity index) is significantly different from those (a null distribution) generated by comparing pseudoreplicated data sets that are drawn at random from pooled empirical occurrence points of the two taxa. The identity test is likely valid only when species tolerate the exact same set of environmental conditions and have the same suite of environmental conditions available to them. Because this is unlikely for allopatric populations, the background test determines whether two taxa are more or less similar than expected based on the differences in the environment background where they occur. This is done by testing the niche similarity index between two taxa against a null distribution for the niche similarity indices between one taxa and random points from the range of the other taxa, and vice versa (i.e., there are actually two null distributions because of the comparisons from two directions; Warren et al., 2010). For the background tests, we divided the large central area of rosefinch distribution into eastern (CWEE) and western (CWEW) groups to account for the large geographic distance involved.

Results

Population structure

The mtDNA network revealed that 9 of the 13 haplotypes from the Caucasus (CA) formed a clade, which was separated by only a few steps from the remaining haplotypes (Fig. 3.2a). The haplotypes in northeastern Eurasia (NEE) were not separated from those in central-western Eurasia (CWE) on the network. Thus, the mtDNA network reveals limited geographic structure. The allele network for ADAMTS6 did not show any geographic structure (Fig. 3.2b). The UPGMA phenogram based on the matrix of mtDNA pairwise Φ_{ST} values showed that the rosefinch populations were clustered into three distinct groups corresponding to CA, NEE, and CWE groups (Fig. 3.3), which is consistent with Pavlova et al.'s (2005) results.

Because the results of the gene tree-based methods suggested two possible group structures, a three-group model and a two-group model, we applied coalescence-based approaches to test which model fits better with the empirical data. The three-group model included the CA, CWE, and NEE. The two-group model consisted of CWE plus NEE (termed ME) and CA. We estimated the demographic parameters associated with the various groupings in the two alternative models and tested them with coalescent simulations.

Analyses of IMa suggested similar evolutionary histories, recent isolation with little or no gene flow followed by population expansion (except for CA), for both the three-group and two-group models. The IMa analyses based on mtDNA and mtDNA plus ADAMTS6 suggested similar histories. We only reported the results based on the latter dataset and used them for simulation. For the three-group model, IMa revealed that

the current population sizes of CWE (7,032,000; 95% credibility interval [CI]= 4,130,000 to 17,303,000) and NEE (616,000; 95% CI= 334,000 to 1,839,000) are significantly larger than those of the ancestral populations (136,000; 95% CI= 58,000 to 240,000), whereas the current population size of CA (167,000; 95% CI= 80,000 to 438,000) was not significantly larger than that of the ancestral population (Fig. 3.4a and b). There was little if any migration between any pair of groups (Fig. 3.4c to e). There could be some migration from NEE to CWE (2×10^{-6} per generation per individual; 95% CI interval= ~0 to 1.6×10^{-5} [we could not reject the possibility of zero gene flow]; Fig. 3.4d). The divergence times between CA and CWE (78,300 years ago; 95% CI= 52,200 to 117,000 years ago), between CWE and NEE (78,800 years ago; 95% CI= 52,000 to 117,200 years ago), and between CA and NEE (76,200 years ago; 95% CI= 42,200 to 141,700 years ago) were similar and recent (Fig. 3.4f). The IMa results for the two-group model revealed that the current population size of ME (8,645,000; 95% CI= 5,396,000 to 18,196,000) was significantly larger than the ancestral population (147,000; 95% CI= 88,000 to 282,000), but that of CA (144,000; 95% CI= 70,000 to 394,000) was not. There was no migration between the two groups and the estimated divergence time (66,400 years ago; 95% CI = 45,500 to 96,600 years ago) was similar to that of the three-group model.

Comparison of the simulated and empirical data supported the three-group model (Fig. 3.5 and 3.6). Because of the uncertainty in gene flow from NEE to CWE (Fig. 3.4d), two three-group models were simulated. One had no gene flow (Fig. 3.5a), and the other had a low level of gene flow (2×10^{-6} per generation per individual) from NEE to CWE (Fig. 3.5b). Given that the dispersal distance of rosefinches is unlikely to span the

entire geographic range, the widely distributed ME (in the two-group model) should not be panmictic. Therefore, we simulated ME by connecting two subgroups with a substantial level of migration, 100 individuals per generation at present but decreasing exponentially backwards in time as the population size decreases (Fig. 3.5c). This level of migration is large enough to prevent population differentiation (Hudson and Coyne, 2002). The ratio of N_e for the two subgroups in ME was 12:1 (Fig. 3.5c) similar to that for CWE and NEE. The Φ_{ST} value of the three groups in the empirical data was within the 95% distribution range of Φ_{ST} values of the three-group model regardless of the level of gene flow (Fig. 3.6a and b) but out of the 95% range of Φ_{ST} values for the two-group (Fig. 3.6c). Therefore, we could reject the two-group but not the three-group model. The similarity between the distributions of Φ_{ST} values for the two three-group models, one with and one without gene flow, suggested that the level of gene flow from NEE to CWE was negligible.

Current and LGM distributions predicted by SDM

The distribution model developed by MAXENT under current climatic conditions predicted the breeding range of common rosefinches including newly colonized areas in Scandinavia (Fig. 3.7a). Although the model predicts occurrence in France, Portugal and Spain the species has not yet become established in these areas, but there are sporadic records (Cramp and Perrins, 1994). Therefore, the predicted current distribution of common rosefinches in Europe was somewhat wider than the observed distribution but consistent with the trend of recent expansion towards the western and northwestern Palearctic (Cramp and Perrins, 1994; Payevsky, 2008).

The predicted distribution at the LGM suggested that common rosefinches mainly occurred in (1) Kamchatka and Magadan, (2) southern Siberia, Mongolia and northern China, and (3) Caucasus (Fig. 3.7b). However, whether the populations in the putative northeastern refugium (i.e., Kamchatka and Magadan) were totally isolated from those in the central refugium (i.e., southern Siberia, Mongolia and northern China) is questionable because of the relatively short gap between them. The LGM distribution also included southern Europe, central China and southern Japan, where the species does not occur at present, and hence no testable predictions can be obtained. Comparing the present and LGM distributions suggests that the Caucasian population has not undergone expansion whereas the other populations expanded westwards since the LGM (Fig. 3.7).

Niche divergence

The niche identity tests (not shown) suggested that the niches of different groups of rosefinches were not identical. For all three comparisons, the niche similarity indices (Schoener's D) of empirical data are significantly smaller than the null distributions generated from pooled occurrence points. However, we found no instances of either niche divergence or niche conservatism in the eight background tests, which took into account the environment available to each group (Fig. 3.8).

Discussion

Our re-analyses of the mtDNA data and analyses of the dataset including new nuclear gene sequences, support the existence of three groups of populations in the common rosefinch, Caucasus, northeastern Eurasia, and central-western Eurasia. These three

groups are not reciprocally monophyletic for either mtDNA or the Z-linked gene tree, suggesting that the rosefinches are at an early stage of diversification and likely speciation. Our estimates of gene flow were essentially zero, indicating that the groups are evolving independently. In addition, the SDM implies that these three groups might have allopatric LGM refugia. Further supporting our hypothesis of the distinctness of these groups, we note that all three groups correspond to named subspecies, *C. e. kubanensis*, *C. e. grebnitskii*, and *C. e. erythrinus* (Cramp and Perrins, 1994; Fig. 3.1). A fourth subspecies, *C.e. ferghanensis*, represented by our Almaty samples was not genetically supported. Nonetheless, these three groups should be considered when forming conservation plans for their respective areas.

Recent history of common rosefinches revealed by phylogeography and SDM

The application of SDM to evolutionary studies is promising (Carnaval et al., 2009; Kozak et al., 2008) although their performance has been under debate (e.g. Araújo et al., 2009; Beale et al., 2008). Our SDM predicted the occurrence of common rosefinches in western Europe even though our model did not incorporate breeding sites from this region. The fact that the species has recently become common in Scandinavia and has bred locally in other European areas (Cramp and Perrins, 1994; Payevsky, 2008), and that the remainder of the predicted range conforms to the known distribution, suggests that our SDM is relatively robust.

In general, it is difficult to determine the geographic locations of LGM refugia, irrespective of whether one uses a SDM or makes inferences from the extant phylogeographic pattern. We consider our SDM and genetic results to be reciprocally

illuminating. Our SDM (Fig. 3.7) is a snapshot at the maximum of the last glacial period, which lasted for ca. 100,000 years (Lisiecki and Raymo, 2007), and it is not straightforward to tell how many refugia might have existed for rosefinches at the LGM. Our genetic results were consistent with three historically isolated groups (Fig. 3.3 and 3.6). Therefore, we suggest that two refugia existed in the eastern Palearctic at the LGM, even though our SDM shows a relatively short gap between them and does not unambiguously reveal their locations. The lack of sorting of mtDNA haplotypes from the Palearctic (excluding CA; Fig. 3.3a) coupled with the inference of negligible gene flow between NEE and CWE (Fig. 3.5), suggests that these two groups became isolated recently. Haploid, non-recombining mtDNA gene trees require isolation lasting approximately N_e generations to reach reciprocal monophyly (Hudson and Coyne 2002). Given the large estimates of N_e for the two main Palearctic groups (7,032,000 and 616,000), considerable time would have to elapse before the mtDNA gene tree would become reciprocally monophyletic. Therefore, our estimate of divergence time for these two groups, 78,800 years ago, suggests that there has been insufficient time for the mtDNA gene tree to evolve to reciprocal monophyly. Given the average N_e of Z-linked genes is three times larger than mtDNA, we expect that the ADSMTS6 gene tree would show less geographic structure than the mtDNA gene tree, which we observed.

Our approaches combining coalescence and SDM analyses allowed additional insight into rosefinch population history. Our analyses revealed that CWE and NEE experienced population expansion, whereas CA did not (Fig. 3.4). However, the degree of expansion for CWE was 10 times greater than that for NEE, and from the SDM it would appear logical given the amount of area into which CWE expanded compared to

NEE. The similarity in range size for the CA group at the present and LGM would lead to the prediction of little if any population increase, which was consistent with the genetic data.

The predicted LGM occurrence of rosefinches in areas south of where they presently occur in southern Europe is relevant to past hypotheses about the distribution of genetic variation following glacial retreat. Hewitt (2004) suggested that genetic variation decreases in the direction of colonization from a refugium owing to sampling effects, termed "leading edge expansion." However, if the refugium no longer has suitable habitat, as is the case for common rosefinches in southern Europe, this prediction is not testable. Thus, a SDM can modify predictions about post-glacial patterns of genetic variation. In this case, one might look to the southern extent of the current range as being the closest to refugial populations, although we lacked data for a strong test of this hypothesis.

The SDM is consistent with a history of isolation for rosefinches in the Caucasus. Compared to CWE and NEE, CA has a relatively smaller effective population size and has not experienced population expansion. These attributes can explain why approximately 70% of haplotypes in CA form a clade in the mtDNA tree (Pavlova et al. 2005) and haplotype network (Fig. 3.2), whereas the other two groups do not. We acknowledge that small sample sizes of the CA group, which were collected from a relatively small geographic area, might contribute to the lack of evidence for population expansion. However, we believe such bias, if it exists, is minor because our SDM (Fig. 3.7) shows a limited LGM as well as current distribution. We predict that if the isolation and current population size continues, the Caucasian population will be the first group to

become a new species. This prediction is supported by the fact that the birds from Caucasus, classified as *C. e. kubanenesis*, are larger and more rosy-red colored than the birds from other parts of their range (Beaman and Madge, 1998; Cramp and Perrins, 1994). This example illustrates that relatively small and isolated populations on islands, continental habitat islands, or mountaintops are potent grounds for lineage diversification.

Niche evolution between the recently diverged common rosefinch groups

The recent separation of the three rosefinch groups makes them appropriate for testing ecological speciation, because the time since isolation is extremely short, and any ecological differences would not likely be attributed to post-isolation divergence. We found no evidence for niche divergence, a result consistent with that for other groups of birds that are considerably more differentiated (Peterson et al., 1999; McCormack et al., 2010). These results of niche identity and background tests reinforce the importance of considering environment availability when testing niche divergence (McCormack et al., 2010).

The use of niche models to examine ecological divergence has recently undergone a series of advancements. For example, if the SDM model of one species does not predict the distribution of a closely related species, one might assume that niche divergence has occurred. Rice et al. (2003) concluded that several taxa of jays (*Aphelacoma*) were ecologically divergent because their niche models did not cross-predict. By contrast, McCormack et al. (2010) found that there was little evidence for ecological divergence when using background tests (Warren et al. 2010). However, it is not clear how to interpret these tests. McCormack et al. (2010) compared four taxa,

resulting in 6 pairwise tests, which are not all independent. The maximum number of either niche conservatism or divergence would be 12. If niche evolution was random, one might expect four cases of conservatism, four of divergence and four showing neither. Their observation of 7, 2 and 3 is consistent with their interpretation that niche divergence is not a major factor, but it is not clear whether it departs from random, nor what the null expectation should be.

In our study, we examined four groups but only did four pairwise tests of niche divergence (to reduce instances of non-independence), finding no instances of niche divergence (or conservatism). Thus, our findings are reminiscent of the jays examined by McCormack et al. (2010). The lack of support for niche divergence or conservatism may indicate that rosefinches, a habitat generalist species, can survive in varied habitats. This may explain the recent population expansion of rosefinches shown by genetic data and current expansion to new ranges in Europe. On the other hand, given the general lack of niche divergence, one might expect that the groups would invade each other's ranges. That is, during the ensuing 21,000 years since the LGM, and a dispersal distance typical for passerine birds of ≥ 1 km per generation (Barrowclough 1980), there would have been ample time for range expansion and homogenization of the three groups. However, our estimates of gene flow suggest this is not occurring. Hence it is possible that the forms exclude each other behaviorally or we have not captured the most important niche dimensions.

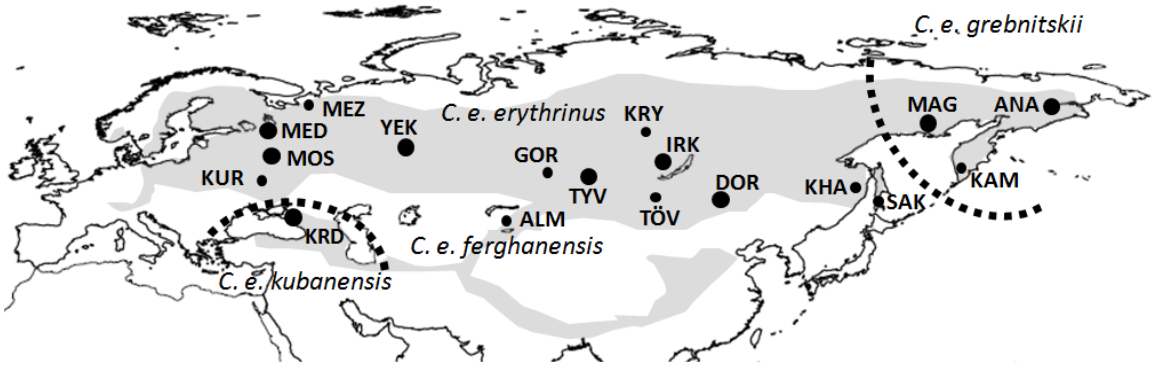

Figure 3.1. Breeding range of the Common Rosefinch (*Carpodacus erythrinus*) with four subspecies indicated and location of sample sites (re-drawn from Fig. 1 in Pavlova et al. 2005). Grey area indicates breeding range. Large solid circles indicate sample sizes of 10 or more individuals. Dotted lines partition the population into three groups as indicated by the pairwise mtDNA Φ_{ST} analysis (Pavlova et al. 2005) and the UPGMA tree based on a matrix of mtDNA Φ_{ST} values (Fig. 3 in this study). ALM is Almaty, ANA is Anadyr', DOR is Dornod, GOR is Gorno-Altay, IRK is Irkutsk, KAM is Kamchatka, KHA is Khabarovsk, KRD is Krasnodar, KRY is Krasnoyarsk, KUR is Kursk, MAG is Magadan, MED is Medvedevo, MEZ Mezen', MOS is Moscow, SAK is Sakhalin, TÖV is Töv, TYV is Tyva, and YEK is Yekaterinburg.

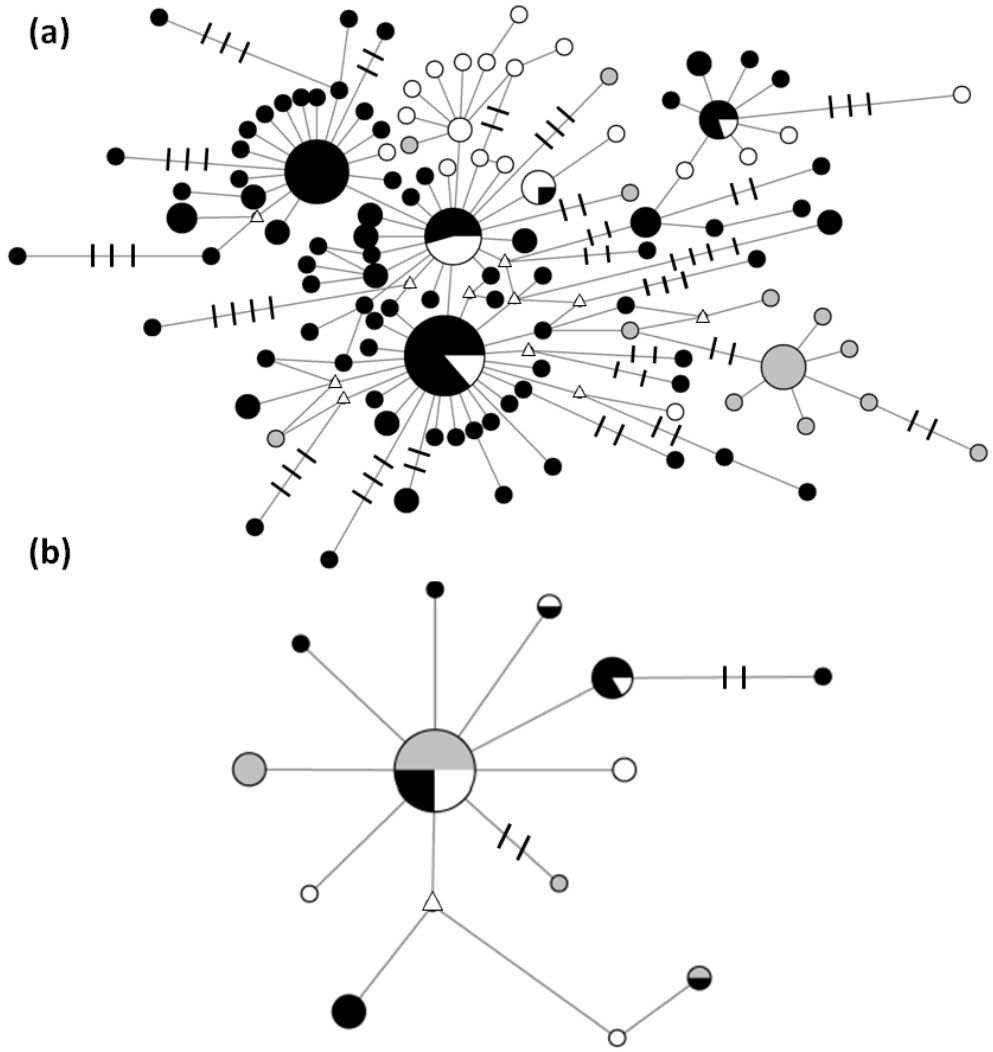

Figure 3.2. Network of (a) mtDNA and (b) a Z-linked intron (ADAMTS6) haplotypes of the common rosefinch by the minimum spaning criterion. Colors on the network indicate the locations at which each haplotype was detected. Black circles indicate center-western Eurasian (CWE) haplotyps, white circles indicate northeastern Eurasian (NEE) ones, and grey circles indicate Caucasian (CA) ones. Open triangles indicate unsampled or extinct haplotypes. Sizes of circles are proportional to haplotype frequencies. Short lines indicate one mutation step.

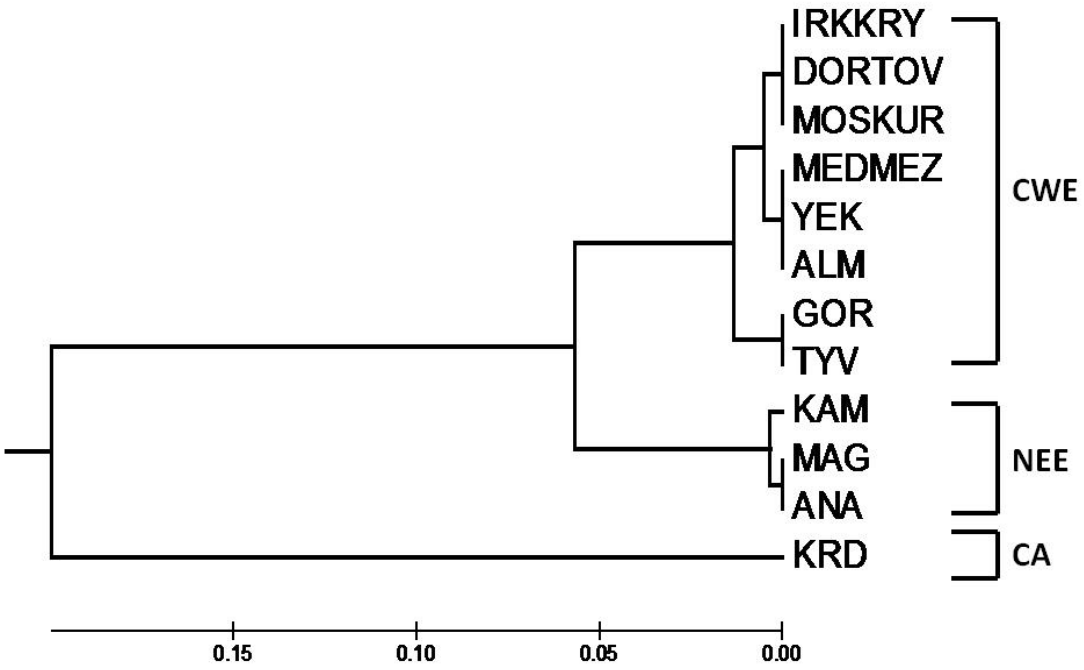

Figure 3.3. UPGMA tree showing relationships among rosefinch population samples. The tree is reconstructed based on the matrix of Φ_{ST} values. The three clades correspond to the center-western Eurasian (CWE), northeastern Eurasian (NEE), and Caucasian (CA) groups. Localities with sample sizes smaller than five were combined with samples in other nearby localities. Therefore, DORTOV is the combination of Dornod and Töv's samples, IRKKRY is that of Irkutsk and Krasnoyarsk, MEDMEZ is that of Medvedevo and Mezen, and MOSKUR is that of Moscow and Kursk. The combined population of Sakhalin and Khabarovsk with only four individuals was excluded from analysis to avoid biases in Φ_{ST} estimates.

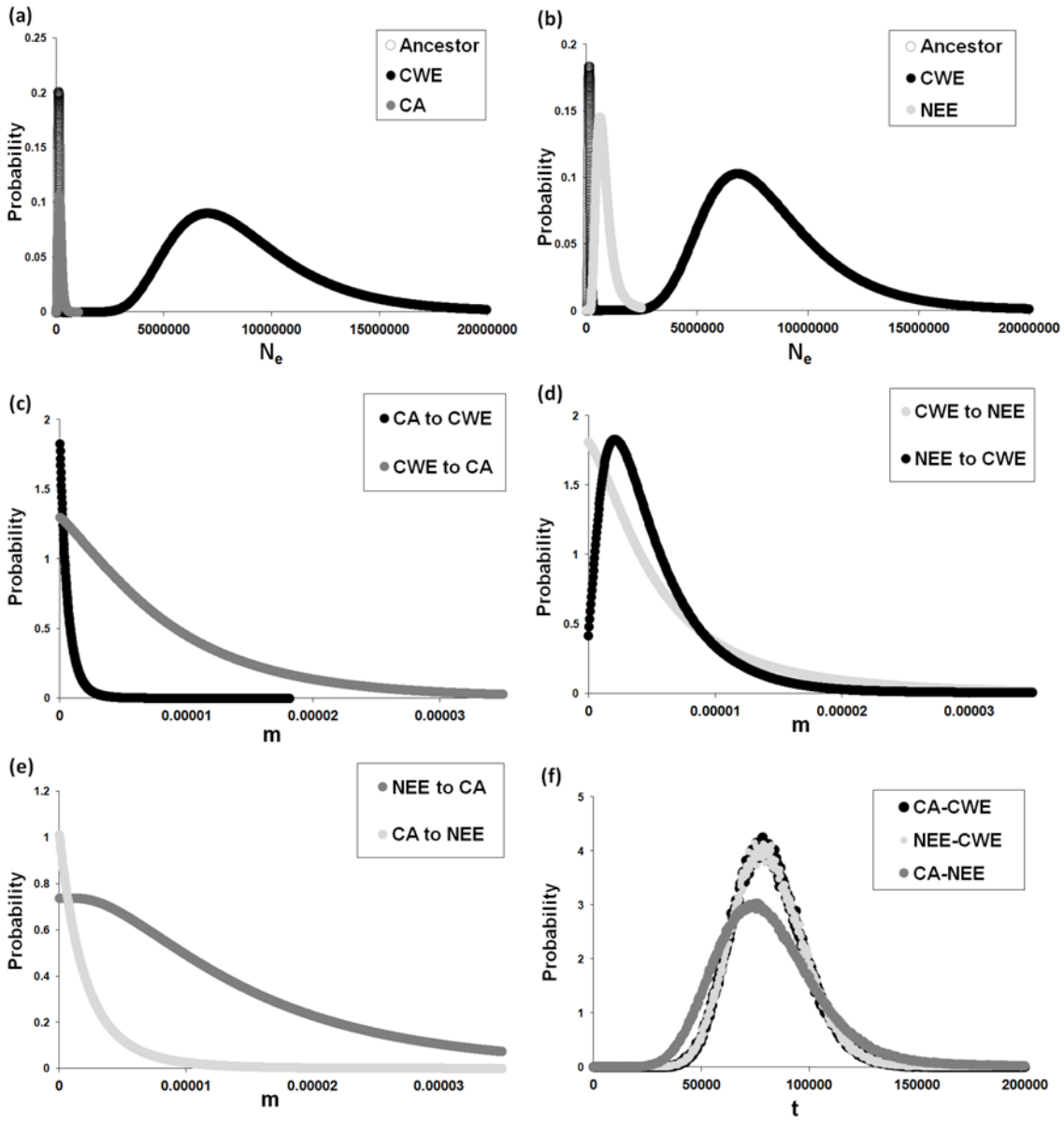

Figure 3.4. The marginal posterior probabilty distribution of the IMa parameters based on mtNDA and a Z-linked intron (ADMATS6) combined for the three-group model. Effective population sizes, θ, for Caucasus (CA), central-western Eurasia (CWE), northeastern Eurasia (NEE) groups and ancestral populations are shown in (a) and (b). Migration rates, *m*, in two directions and divergence times, *t*, between CA and CWE, between CWE and NEE, and between CA and NEE are shown in (c) to (f).

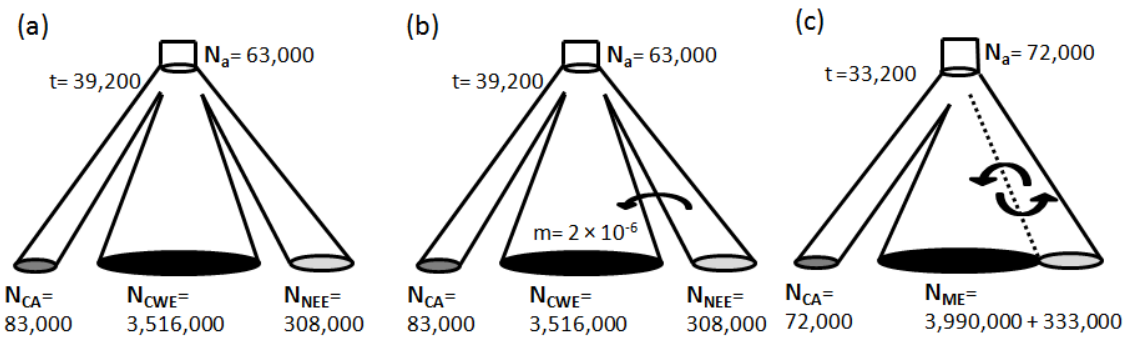

Figure 3.5. Outline of the three-group models (a and b) and the two-group model (c) developed to test hypothesized demographic histories for the commone Rosefinch. N_a, N_{CA}, N_{CWE}, N_{NEE}, and N_{ME} indicate effecive population sizes of ancestral, CA, CWE, NEE, and ME groups, respectively. t indicates time of divergence in units of generations from present. Arrows indicate gene flow. The immigration rate (m) in the (b) model is shown in the figure. The levels of gene flow in the (c) model are 100 immigrants per generation currently but decrease exponentially backwards in time as the population sizes decrease. The dashed lines indicate that the groups are connected to each other with substantial levels of gene flow.

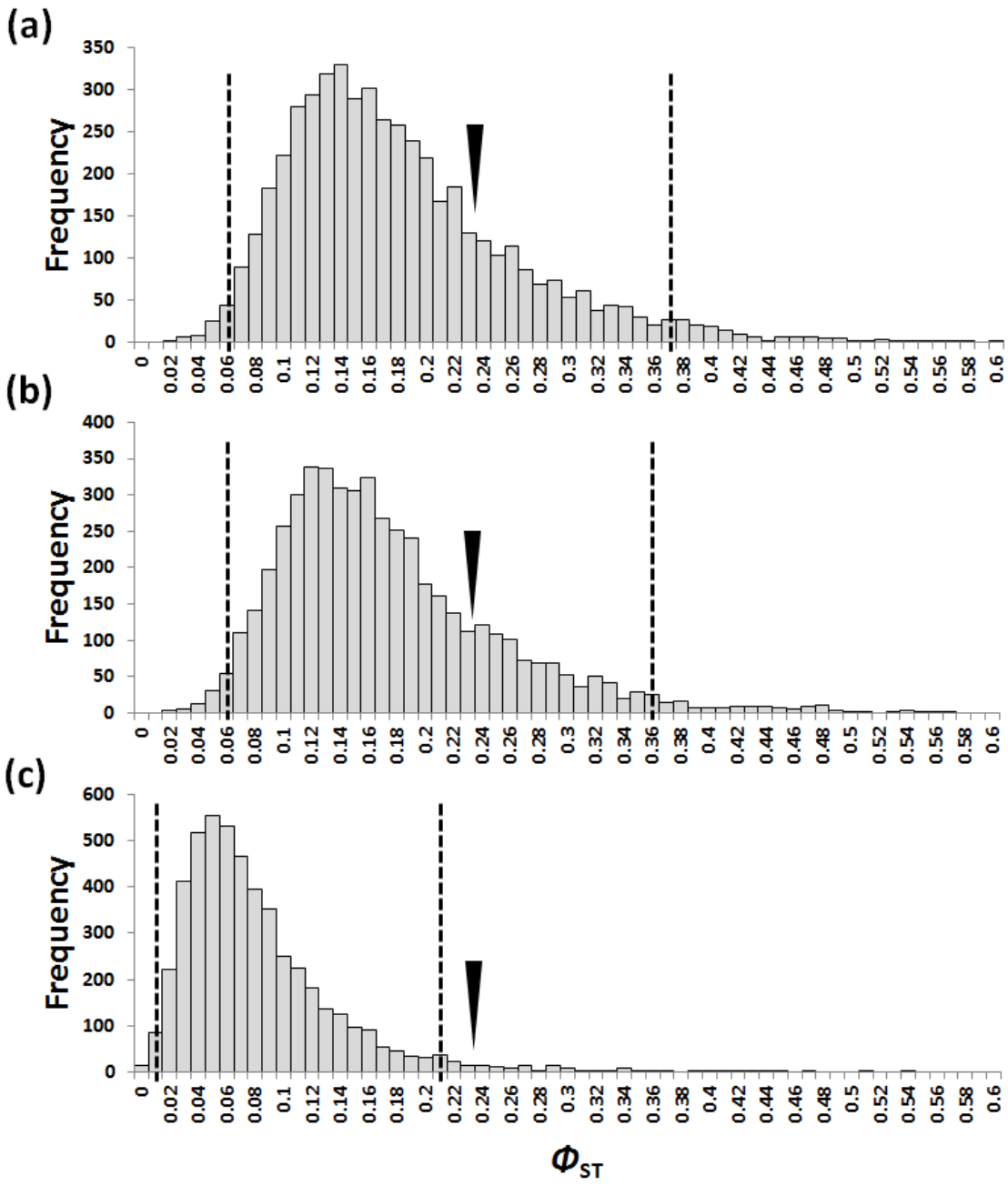

Figure 3.6. Histograms of Φ_{ST} values for 5000 simulated sequence data sets. (a) Results from simulations of the three-group model without gene flow. (b) Results from simulation of the three-group model with a low level of gene flow from NEE to CWE. (c) Results from simulations of the two-group model. The dashed lines represent the 2.5 and 97.5 percentiles in the distribution. The black triangles represent the Φ_{ST} value of our empirical data.

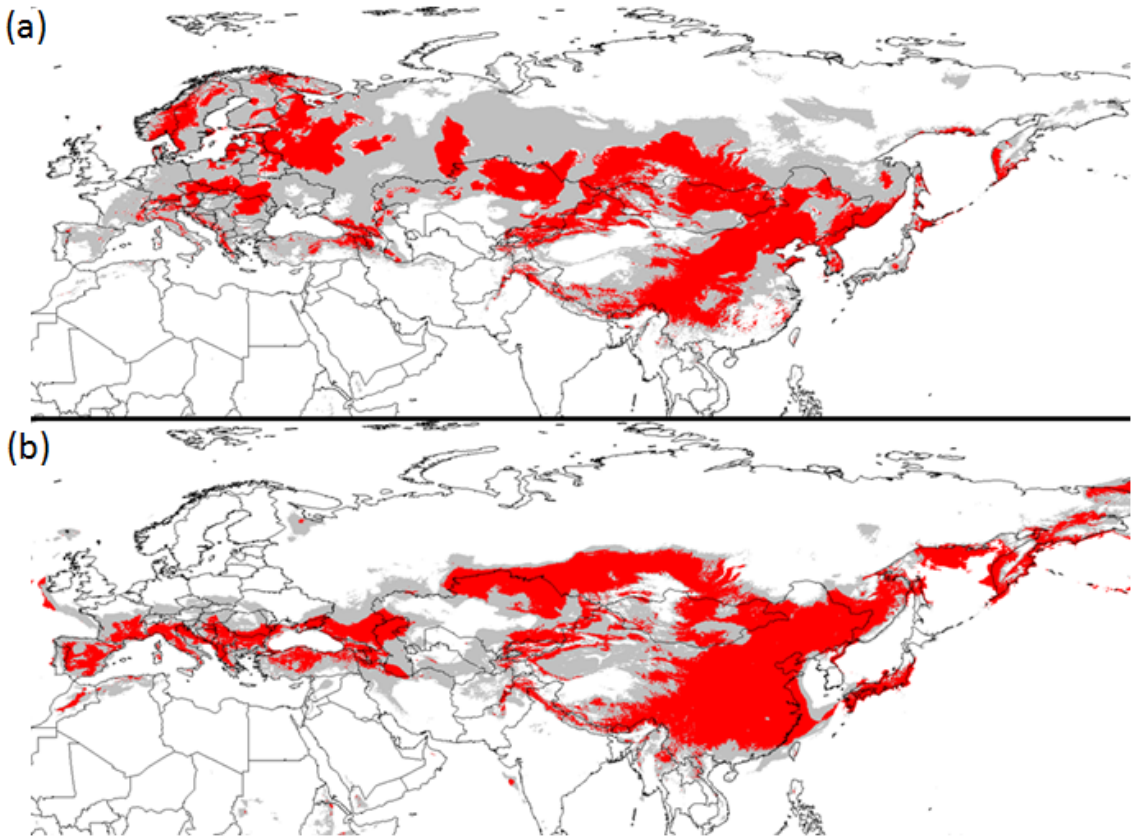

Figure 3.7. Predicted distributions of the common rosefinch (*Carpodacus erythrinus*) for (a) present and (b) LGM conditions using MAXENT.

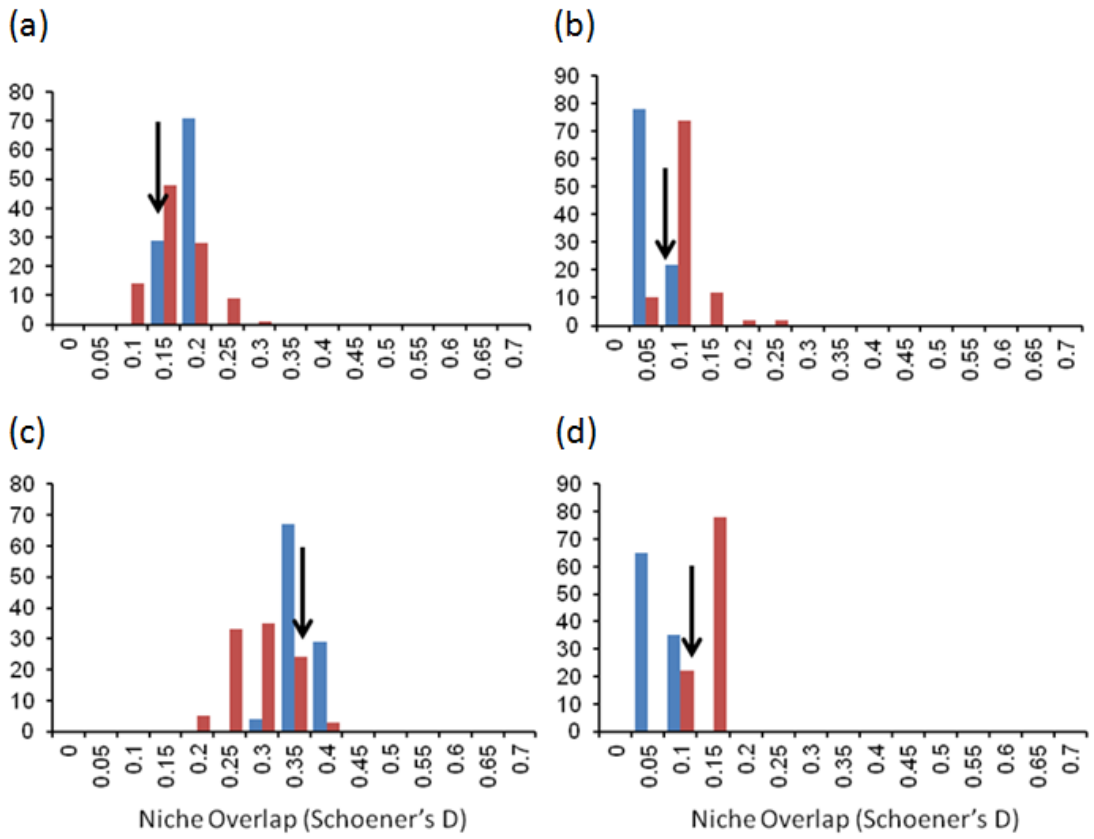

Figure 3.8. Background tests for niche divergence. Arrows indicate niche similarity index (Schoener's D) between two groups and are compared with a null distribution for the niche similarity indices between one group and random points from the range of the other group and vice versa. (a) Blue histogram indicates a null distribution of NEE versus the background of CWEE, and red indicates the opposite comparison. (b) Blue indicates a null distribution of CA versus the background of NEE, and red indicateds the opposite comparison. (c) Blue indicates a null distribution of CA versus the background of CWEW, and red indicateds the opposite comparison. (d) Blue indicates a null distribution of CWEE versus the background of CWEW, and red indicates the opposite comparison. Niche similarity values smaller than a null distribution indicate niche divergence, larger values indicate niche conservatism, and values within a null distrubiton indicate neither niche divergence nor niche conservatism.

Bibliography:

Abbott, R. J., and C. Brochmann. 2003. History and evolution of the arctic flora: in the footsteps of Eric Hultén. Mol. Ecol. 12:299-313.

Adams, J. M. 2002. Global land environments since the last interglacial. Available at http://www.esd.ornl.gov/projects/qen/nerc.html

Alfaro, M. E., S. Zoller, and F. Lutzoni. 2003. Bayes or bootstrap? A simulation comparing the performance of Bayesian Markov Chain Monte Carlo sampling and bootstrapping in assessing phylogenetic confidence. Mol. Biol. Evol. 20:255-266.

Araújo, M. B., W. Thuiller, and N. Yoccoz. 2009. Reopening the climate envelope reveals macroscale associations with climate in European birds. Proc. Natl. Acad. Sci. USA 106:E45-E46.

Arbogast, B. S., S. V. Drovetski, R. L. Curry, P. T. Boag, G. Seutin, P. R. Grant, B. R. Grant, and D. J. Anderson. 2006. The origin and diversification of Galapagos mockingbirds. Evolution 60:370-382.

Arnold, K., L. Bordoli, J. Kopp, and T. Schwede. 2006. The SWISS-MODEL Workspace: A web-based environment for protein structure homology modeling. *Bioinformatics* 22:195-201.

Avise, J. C. 2000. Phylogeography: the history and formation of species. Harvard Univ. Press, Cambridge, MA.

Avise, J. C., J. Arnold, R. M. Ball, E. Bermingham, T. Lamb, J. E. Neigel, C. A. Reeb, and N. C. Sauders. 1987. Intraspecific phylogeography: the mitochondrial DNA bridge between population genetics and systematics. Annu. Rev. Ecol. Sys. 18:489-522.

Backström, N., M. Brandström, L. Gustafsson, A. Qvarnström, H. Cheng, and H. Ellegren. 2006. Genetic mapping in a natural population of collared flycatchers (*Ficedula albicollis*): conserved synteny but gene order rearrangements on the avian z chromosome. Genetics 17:377-386.

Backström, N., S. Fagergerg, and H. Ellegren. 2008. Genomics of natural bird populations: a gene-based set of reference markers evenly spread across the avian genome. Mol. Ecol. 17:964-980.

Ballard, J. W. O., and R. G. Melvin. 2010. Linking the mitochondrial genotype to the organismal phenotype. Mol. Ecol. 19:1523-1539.

Ballard, J. W. O, and M. C. Whitlock. 2004. The incomplete natural history of mitochondria. Mol. Ecol. 13:729-744.

Bandelt, H.-J., P. Forster, and A. Röhl. 1999. Median-joining networks for inferring intraspecific phylogenies. Mol. Biol. Evol. 16:37-48.

Barker, F. K., A. J. Vandergon, and S. M. Lanyon. 2008. Assessment of species limits among yellow-breasted meadowlarks (*Sturnella* spp.) using mitochondrial and sex-linked markers. Auk 125:869-879.

Barrowclough, G.F. 1980. Genetic and phenotypic differentiation in a wood warbler (genus *Dendroica*) hybrid zone. Auk 97:655-668.

Bazin, E., S. Glémin, and N. Galtier. 2006. Population size does not influence mitochondrial genetic diversity in animals. Nature 312:570-572.

Beale, C. M., J. J. Lennon, and A. Gimona. 2008. Opening the climate envelope reveals no macroscale associations with climate in European birds. Proc. Natl. Acad. Sci. USA 105:14908-14912.

Beaman, M., and S. Madge. 1998. The Handbook of bird identification for Europe and the Western Palearctic. Princeton University Press, Princeton.
Beheregaray, L. B. 2008. Twenty years of phylogeography: the state of the field and the challenges for the Southern Hemisphere. Mol. Ecol. 17:3754-3774.
Bensch, S., D. E. Irwin, J. H. Irwin, L. Kvist, and S. Åkesson. 2006. Conflicting patterns of mitochondrial and nuclear DNA diversity in *Phylloscopus* warblers. Mol. Ecol. 15:161-171.
Berlin, S., D. Tomaras, and B. Charlesworth. 2007. Low mitochondrial variability in birds may indicate Hill-Roberson effects on the W chromosome. Heredity 99:389-396.
Birky, C. W. J. 1991. Evolution and population genetics of organelle genes: mechanisms and models. Pp. 112-134. *In* R. K. Selander, A. G. Clark, and T. S. Whittam (eds.). Evolution at the molecular level. Sinauer Associates, Sunderland, MA.
Bossu, C. M., and T. J. Near. 2009. Gene trees reveal repeated instances of mitochondrial DNA introgression in orangethroat darters (Percidae: *Etheostoma*). Syst. Biol. 58:114-129.
Boutin-Ganache, I., M. Raposo, M. Raymond, and C. F. Deschepper. 2001. M13-tailed primers improve the readability and usability of microsatellite analyses performed with two different allele sizing methods. Biotechniques 31:24-27.
Brelsford, A., and D. Irwin. 2009. Incipient speciation despite little assortative mating: the yellow-ramped warbler hybrid zone. Evolution 63:3050-3060.
Brito, P. H., and S. V. Edwards. 2009. Multilocus phylogeography and phylogenetics using sequence-based markers. Genetica 135:439-455.
Busch, J. W., S. Joly, and D. J. Schoen. 2011. Demographic signatures accompanying the evolution of selfing in *Leavenworthia alabamica*. Mol. Biol. Evol. 28:1717-1729.
Carnaval, A. C., M. J. Hickerson, C. F. B. Haddad, M. T. Rodrigues, and C. Moritz. 2009. Stability predicts genetic diversity in the Brazilian Atlantic forest hotspot. Science, 323:785-789.
Carstens, B. C., and L. L. Knowles. 2007. Estimating species phylogeny from gene-tree probabilities despite incomplete lineage sorting: an example from *Melanoplus* grasshoppers. Syst. Biol. 56:400-411.
Castoe, T. A., Z. J. Jiang, W. Gu, Z. O. Wang, and D. D. Pollock. 2008. Adaptive evolution and functional redesign of core metabolic protein in snakes. PLoS ONE 3: e2201. doi:10.1371/journal.pone.0002201.
Calvignac, S., L. Konecn, F. Malard, and C. J. Douady. 2011. Preventing the pollution of mitochondrial datasets with nuclear mitochondrial paralogs (numts). Mitochondrion 11:246-254.
Carling, M. D., and R. T. Brumfield. 2008. Haldane's rule in an avian system: using cline theory and divergence population genetics to test for differential introgression of mitochondrial, autosomal, and sex-linked loci across the *Passerina* hunting hybrid zone. Evolution 62:2600-2615.
Clark, A. G. 1990. Inference of haplotypes from PCR-amplified samples of diploid populations. Mol. Biol. Evol. 7:111-122.
Clarke, A. L., B. E. Sæther, and E. Røskaft. 1997. Sex biases in avian dispersal: a reappraisal. Oikos 79:429-438.
Cramp, S., and C. M. Perrins. 1994. Handbook of the Birds of Europe, the Middle East and North Africa, vol. 5. Oxford University Press, Oxford.

Crow, J., and M. Kimura. 1970. An introduction to population genetic theory. Burgess Publishing Company, Minneapolis, MN.
Dolman, G., and C. Moritz. 2006. A multilocus perspective on refugial isolation and divergence in rainforest skinks (*Carlia*). Evolution 60:573-582.
Dowling, D., U. Friberg, and J. Lindell. 2008. Evolutionary implications of non-neutral mitochondrial genetic variation. Trends Ecol. Evol. 23:546-554.
Drovetski, S. V., R. M. Zink, I. V. Fadeev, Y. V. Nesterov, Y. A. Koblik, Y. A. Red'kin, and S. Rohwer. 2004. Mitochondrial phylogeny of *Locustella* and related genera. J. Avian Biol. 35:105-110.
Drovetski, S.V., R. M. Zink, S. R. Rohwer, I. V. Fadeev, E. V. Nesterov, I. Karagodin, E. A. Koblik, and Y. A. Red'kin. 2004. Complex biogeographic history of a Holarctic passerine. Proc. R. Soc. Lond. B 271:545-551.

Drovetski, S. V., R. M. Zink, P. G. P. Ericson, and I. V. Fadeev. 2010. A multi-locus study of pine grosbeak phylogeography supports the pattern of greater intercontinental divergence in Holarctic boreal forest birds compared to birds inhabiting other high-latitude habitats. J. Biogeogr. 37:696-706.
Drummond, A. J., and A. Rambaut. 2007. BEAST: Bayesian evolutionary analysis by sampling trees. BMC Evol. Biol. 7:214. doi:10.1186/1471-2148-7-214.
Edwards, S., and S. Bensch. 2009. Looking forwards or looking backwards in avian phylogeography? A comment on Zink and Barrowclough 2008. Mol. Ecol. 18:2930-2933.
Ellegren, H. 2007. Molecular evolutionary genomics of birds. Cytogenet. Genome Res. 117:120-130.
EPICA. 2004. Eight glacial cycles from an Antarctic ice core. Nature 429:623-628.
Evanno G., S. Regaut, and J. Goudet. 2005. Detecting the number of clusters of individuals using the software STRUCTUER: a simulation study. Mol. Ecol. 14:2611-2620.
Excoffier, L., P. Smouse, and J. Quattro. 1992. Analysis of molecular variance inferred from metric distances among DNA haplotypes: Application to human mitochondrial DNA restriction data. Genetics 131:479-491.
Fedorov, V. B., A. V. Goropashnaya, G. G. Boeskorov, and J. A. Cook. 2008. Comparative phylogeography and demographic history of the wood lemming (*Myopus schisticolor*): implications for late Quaternary history of the taiga species in Eurasia. Mol. Ecol. 17:598-610.
Friesen, V. L., B. C. Congdon, M. G. Kidd, and T. P. Birt. 1999. Polymerase chain reaction (PCR) primers for the amplification of five nuclear introns in vertebrate. Mol. Ecol. 8:2147-2149.
Funk, D. J. and K. E. Omland. 2003. Species-level paraphyly and polyphyly: frequency, causes, and conseqeunces, with insights form animal mitochondrial DNA. Annu. Rev. Ecol. Syst. 34:397-423.
Galtier, N., B. Nabholz, S. Glémin, and G. D. D. Hurst. 2009. Mitochondrial DNA as a marker of molecular diversity: a reappraisal. Mol. Ecol. 18:4541-4550.
Gershoni, M., A. R. Templeton, and D. Mishmar. 2009. Mitochondrial bioenergetics as a major motive force of speciation. BioEssays 31:642-650.

Gibbard, P., and T. Van Kolfschoten. 2004. The Pleistocene and Holocene Epochs. *In* F. M. Gradstein, J. G. Ogg, A. G. Smith (eds.). A geologic time scale. Cambridge University Press, London.
Gillespie, J. H. 2000. Genetic drift in an infinite population: the pseudohitchhiking model. Genetics 155:909-919.
Gillespie, J. H. 2001. Is the population size of a species relevant to its evolution? Evolution 55:21161-2169.
Guex, N., and M. C. Peitsch. 1997. SWISS-MODEL and the Swiss-PdbViewer: An environment for comparative protein modeling. Electrophoresis 18:2714-2723.
Hackett, S. J. 1996. Molecular phylogenetics and biogeography of tanagers in the genus Ramphocelus (Aves). Mol. Phylogenet. Evol. 5:368-382.
Hahn, M. W. 2008. Toward a selection theory of molecular evolution. Evolution 62:255-265.
Haldane, J. B. S. 1922. Sex ratio and unisexual sterility in animal hybrids. J. Genet. 12:101-109.
Haring, E., A. Gamauf, and A. Kryukov. 2007. Phylogeographic patterns in widespread corvid birds. Mol. Phyl. Evol. 45:840-862.
Harshman, J. 1996. Phylogeny, evolutionary rates, and ducks. Ph.D. dissertation, University of Chicago, Chicago.
Head, M. J., P. Gibbard, and A. Salvador. 2008. The Quaternary: its character and definition. Episodes 31:234-238.
Heled, J., and A. J. Drummond. 2008. Bayesian inference of population size history from multiple loci. BMC Evol. Biol. 8:289. doi:10.1186/1471-2148-8-289.
Heled, J., and A. J. Drummond. 2010. Bayesian inference of species trees from multilocus data. Mol. Biol. Evol. 27:570-580.
Herman, J. S., and J. B. Searle. 2011. Post-glacial partitioning of mitochondrial genetic variation in the field vole. Proc. R. Soc. B 278:3601-3607.
Hewitt, G. M. 2000. The genetic legacy of the Quaternary. Nature 405:907-913.
Hewitt, G. M. 2004. Genetic consequences of climatic oscillations in the Quaternary. Philos. T. Roy. Soc. B 359:183-195.
Hey, J., and R. Nielsen. 2004. Multilocus methods for estimating population sizes, migration rates and divergence time, with applications to the divergence of *Drosophila pseudoobscura* and *D. persimilis*. Genetics 167:747-760.
Hey, J., and R. Nielsen. 2007. Integration within the Felsenstein equation for improved Markov chain Monte Carlo methods in population genetics. Proc. Natl. Acad. Sci. USA 104:2785-2790.
Hey, J. 2010. Isolation with migration models for more than two populations. Mol. Biol. Evol. 27:905-920.
Hickerson, M. J., B. C. Carsten, J. Cavender-Bares, K. A. Crandall, C. H. Graham, J. B. Johnson, L. Rissler, P. F. Victoriano, and A. D. Yoder. 2010. Phylogeography's past, present, and future: 10 years after Avise, 2000. Mol. Phyl. Evol. 54:291-301.
Hijmans, R. J., L. Guarino, C. Bussink, P. Mathur, M. Cruz, I. Barrentes, and E. Rojas. 2004. DIVA-GIS. Vsn. 7.1.7. A geographic information system for the analysis of species distribution data. Manual available at http://www.diva-gis.org

Hijmans, R. J., S. E. Cameron, J. L. Parra, P. G. Jones, A. Jarvis. 2005. Very high resolution interpolated climate surfaces for global land areas. Int. J. Climatol. 25:1965-1978.

Ho, S. Y. W., J. P. Matthew, A. Cooper, and A. J. Drummond. 2005. Time dependency of molecular rate estimates and systematic overestimation of recent divergence times. Mol. Biol. Evol. 22:1561-1568.

Hoekstra, H., R. J. Hirschmann, R. A. Bundey, P. A. Insel, and J. P. Crossland. 2006. A single amino acid mutation contributes to adaptive beach mouse color pattern. Science 313:101-104.

Hudson, R. R., and J. A. Coyne. 2002. Mathematical consequences of the genealogical species concept. Evolution 56:1557-1665.

Hudson, R. R., M. Kreitman, M. Aguadé. 1987. A test of neutral molecular evolution based on nucleotide data. Genetics 116:153-159.

Hudson, R. R., and M. Turelli. 2003. Stochasticity overrules the 'three-times rule': genetic drift, genetic draft, and coalescence times for nuclear loci versus mitochondrial DNA. Evolution 57:182-190.

Hughes, A. L. 2007. Looking for Darwin in all the wrong places: the misguided quest for positive selection at the nucleotide sequence level. Heredity 99:364-373.

Hughes, A. L., and A. K. Hughes. 2007. Coding sequence polymorphism in avian mitochondrial genomes reflects population histories. Mol. Ecol. 16:1369-1376.

Jennings, W. B., and S. Edwards. 2005. Speciational history of Australian grass finches (*Poephila*) inferred from thirty gene trees. Evolution 59:2033-2047.

Jones, D. T., W. R. Taylor, and J. M. Thornton. 1994. A model recognition approach to the prediction of all-helical membrane protein structure and topology. Biochemistry 33:3038–3049.

Kerr, K. C. R. 2011. Searching for evidence of selection in avian DNA barcodes. Mol. Ecol. Resour. 11:1045-1055.

Kimball, R.T., E. L. Braun, and F. K. Barker et al. (20 co-authors) 2009. A well-tested set of primers to amplify regions spread across the avian genome. Mol. Phyl. Evol. 50:654-660.

Kimura, M. 1968. Evolutionary rate at the molecular level. Nature 217:624-626.

Kimura, M. 1969. The number of heterozygous nucleotide sites maintained in a finite population due to steady flux of mutations. Genetics 61:893-903.

Kimura, M. 1983. The neutral theory of molecular evolution. Cambridge: Cambridge University Press.

Klicka, J. G. Spellman, K. Winker, V. Chua, and B. Smith. 2011. A phylogeographic and population genetic analysis of a widespread, sedentary North American bird: the Hairy Woodpecker (*Picoides villosus*). Auk 128:346-362.

Knowles, L. L. 2009. Statistical phylogeography. Ann. Rev. Ecol. Evol. Sys. 40:593-612.

Knowles, L. L., and D. F. Alvarado-Serrano. 2010. Exploring the population genetic consequences of the colonization process with spatio-temporally explicit models: insights from coupled ecological, demographic and genetic models in montane grasshoppers. Mol. Ecol. 19:3727-3745.

Knowles, L. L., and B. C. Carstens. 2007. Delimiting species without monophyletic gene trees. Syst. Biol. 56:887-895.

Kocher, T.D., W. K. Thomas, A. Meyer, S. V. Edwards, S. Paabo, F. X. Villablanca, A. C. Wilson. 1989. Dynamics of mitochondrial DNA evolution in animals: Amplification and sequencing with conserved primers. Proc. Natl. Acad. Sci. USA. 86:6196-6200.

Kozak, K. H., C. H. Graham, and J. J. Wiens. 2008. Integrating GIS-based environmental data into evolutionary biology. Trends Ecol. Evol. 23:141-148.

Kubatko, L. S., H. L. Gibbs, and E. W. Bloomquist. 2011. Inferring species-level phylogenies and taxonomic distinctiveness using multilocus data in *Sistrurus* rattlesnakes. Syst. Biol. 60:393-409.

Laval, G., and L. Excoffier. 2004. SIMCOAL 2.0: a program to simulate genomic diversity over large recombining regions in a subdivided population with a complex history. Bioinformatics 20:2485-2487.

Lee, J. Y., and S. V. Edwards. 2008. Divergence across Australia's Carpentarian barrier: statistical phylogeography of the red-backed fairy wren (*Malurus melanocephalus*). Evolution 62:3117-3134.

Li, N., and M. Stephens. 2003. Modelling linkage disequilibrium, and indentifying recombination hotspots using SNP data. Genetics 165:2213-2233.

Librado, P., and J. Rozas. 2009. DnaSP v5: A software for comprehensive analysis of DNA polymorphism data. Bioinformatics 25:1451-1452.

Lim, H. C., and F. H. Sheldon. 2011. Multilocus analysis of the evolutionary dynamics of rainforest bird populations in Southeast Asia. Mol. Ecol. 20:3414-3438.

Lisiecki, L. E., and M. Raymo. 2007. Plio-Pleistocene climate evolution: trends and transitions in glacial cycle dynamics. Quaternary Sci. Rev. 26:56-69.

Lovette, I. J. 2004. Mitochondrial dating and mixed support for the "2% Rule" in birds. Auk 121: 1-6.

MacDougall-Shackleton, E. A., L. Blanchard, and H. L. Gibbs. 2003. Unmelanized plumage patterns in old world leaf warblers do not correspond to sequence variation at the Melanocortin-1 Receptor locus (MC1R). Mol. Biol. Evol. 20:1675-1681.

Maddison, W. P. 1997. Gene trees in species trees. Syst. Biol. 46:523-536.

Maddison, W. P., and L. L. Knowles. 2006. Inferring phylogeny despite incomplete lineage sorting. Syst. Biol. 55:21-30.

Manthey, J. D., J. Klicka, and G. M. Spellman. 2011. Isolation-driven divergence: speciation in a widespread North American songbird (Aves: Certhiidae). Mol. Ecol. 20:4371-4384.

Marmi, J., F. López-Giráldez, D. W. Macdonald, F. Calafell, E. Zholnerovskaya, and X. Domingo-Roura. 2006. Mitochondrial DNA reveals a strong phylogeographic structure in the badger across Eurasia. Mol. Ecol. 15:1007-1020.

Maynard Smith, J. 1987. On the equality of origin and fixation times in genetics. J. Theor. Biol. 128:247-252.

Maynard-Smith, J., and J. Haigh. 1974. The hitch-hiking effect of a favourable gene. Genet. Res. 23:23-35.

McCormack, J. E., A. L. Zellmer, and L. L. Knowles. 2010. Does niche divergence accompany allopatric divergence in *Aphelocoma* jays as predicted under ecological speciation?: insights from tests with niche models. Evolution 64:1231-1244.

McDonald, J. H., and M. Kreitman. 1991. Adaptive protein evolution at the *Adh* locus in *Drosophila*. Nature 351:652-654.

Meiklejohn, C.D., K. L. Montooth, and D. M. Rand. 2007. Positive and negative selection on the mitochondrial genome. Trends Genet. 23:259-263.
Mitrus, C. 2006. The influence of male age and phenology on reproductive success of the red-breasted flycatcher (*Ficedula parva* Bechst.). Ann. Zool. Fennici 43:358-365.
Mitrus, C. 2007. Male aggressive behaviour and the role of delayed plumage maturation in the red-breasted flycatcher Ficedula parva (Bechstein, 1792) during the breeding season. Biological Lett. 44:51-59.
Nei, M. 1987. Molecular evolutionary genetics. Columbia Univ. Press, New York.
Nei, M., and T. Maruyama, and R. Chakraborty. 1975. The bottleneck effect and genetic variability in populations. Evolution 29:1-10.
Nielsen, R. 2005. Molecular signatures of natural selection. Ann. Rev. Genet. 39:197-218.
Nunney, L. 1993. The influence of mating system and overlapping generations on effective population size. Evolution 47:1329-1341.
Oliveira, D. C. S., R. Raychoudhury, D. V. Lavrov, and J. H. Werren. 2007. Rapidly evolving mitochondrial genome and directional selection in mitochondrial genes in the parasitic wasp *Nasonia* (Hymenoptera: Pteromalidae). Mol. Biol. Evol. 25:2167-2180.
Outlaw, D. C., and G. Voelker. 2006. Systematics of *Ficedula* flycatchers (Muscicapidae): A molecular reassessment of a taxonomic enigma. Mol. Phylogenet. Evol. 41:118-126.
Palumbi, S. R., F. Cipriano, and M. P. Hare. 2001. Predicting nuclear gene coalescence from mitochondrial data: the three-times rule. Evolution 55:859-868.
Pastene, L. A., M. Goto, N. Kanda, A. N. Zerbini, D. Kerem, K. Watanabe, Y. Bessho, M. Hasegawa, R. Nielsen, F. Larsen, and P. J. Palsbøll. 2007. Radiation and speciation of pelagic organisms during periods of global warming: the case of the common minke whale, Balaenoptera acutorostrata. Mol. Ecol. 16:1481-1495.
Pavlova, A., R. M. Zink, and S. Rohwer. 2005. Evolutionary history, population genetics, and gene flow in the common rosefinch (*Carpodacus erythrinus*). Mol. Phyl. Evol. 36:669-681.
Payevsky, V. A. 2008. Breeding and demographic parameters and range expansion of the common rosefinch (*Carpodacus erythrinus*). Ring 30:63-69.
Peters, J.L., T. E. Roberts, K. Winker, and K. G. McCracken. 2012. Heterogeneity in genetic diversity among non-coding loci fails to fit neutral coalescent models of population history. PLoS ONE 7:e31972. doi:10.1371/journal.pone.0031972.
Peterson, A. T., J. Sobersón, and V. Sánchez-Cordero. 1999. Conservatism of ecological niches in evolutionary time. Science 285:1265-1267.
Pereira, S.L., and A. Baker. 2004a. Vicariant speciation of Curassows (Aves, Cracidae): a hypothesis based on mitochondrial DNA phylogeny. Auk 121:682-694.
Pereira, S.L., and A. Baker. 2004b. Low number of mitochondrial pseudogenes in the chicken (*Gallus gallus*) nuclear genome: implications for molecular inference of population history and phylogenetics. BMC Evol. Biol. 4:17. doi:10.1186/1471-2148-17.
Phillips, S. J., R. P. Anderson, and R. E. Schapire. 2006. Maximum entropy modeling of species geographic distributions. Ecol. Modell. 19:231-259.
Pielou, E.C. 1979. Biogeography. John Wiley and Sons, New York, NY.

Polzin, T., and S. V. Daneschmand. 2003. On Steiner trees and minimum spanning trees in hypergraphs. Oper. Res. Lett. 31:12-20.
Posada, D., and K. A. Crandall. 1998. MODELTEST: testing the model of DNA substitution. Bioinformatics 14:817-818.
Primmer, C. R., T. Borge, J. Lindell, and G.-P. S□tre. 2002. Single-nucleotide polymorphism characterization in species with limited available sequence information: high nucleotide diversity revealed in the avian genome. Mol. Ecol. 11:603-612.
Pritchard, J. K., M. Stephens, and P. Donnelly. 2000. Inference of population structure using multilocus genotype data. Genetics 155:945-959.
Posada, D. 2008. jModelTest: phylogenetic model averaging. Mol. Biol. Evol. 25:1253-1256.
Rambaut, A., and A. J. Drummond. 2007. Tracer v1.5. Available at http://tree.bio.ed.ac.uk/software/tracer/
Rice, N. H., E. Martínez-Meyer, and A. T. Perterson. 2003. Ecological niche differentiation in the *Aphelocoma* jays: a phylogenetic perspective. Biol. J. Linn. Soc. 80:369-383.
Ronquist, F., and J. P. Huelsenbeck. 2003. MrBayes 3: Bayesian phylogenetic inference under mixed models. Bioinformatics 19:1572-1574.
Rosenberg, N. A. 2004. Distruct: a program for the graphical display of population structure. Mol. Ecol. Notes 4:137-138.
Rosenberg, N., and M. Nordborg. 2002. Genealogical trees, coalescent theory and the analysis of genetic polymorphisms. Nat. Rev. Genet. 3:380-390.
Rovito, S. M. 2010. Lineage divergence and speciation in the Web-toed Salamanders (Plethodontidae: *Hydromantes*) of the Sierra Nevada, California. Mol. Ecol. 19:4554-4571.
Salzburger, W., J. Martens, A. A. Nazarenko, Y.-H. Sun, R. Dallinger, and C. Sturmbauer. 2002 Phylogeography of the Eurasian Willow Tit (Parus montanus) based on DNA sequences of the mitochondrial cytochrom *b* gene. Mol. Phyl. Evol. 24:26-34.
Sangster, G., P. Alström, E. Forsmark, and U. Olsson. 2010. Multi-locus phylogenetic analysis of Old World chats and flycatchers reveals extensive paraphyly at family, subfamily and genus level (Ave: Muscicapidae*). Mol. Phylogenet. Evol.* 57:380-392.
Schluter, D. 2009. Evidence for ecological speciation and its alternative. Science 323:737-741.
Schneider, S., D. Roessli, and L. Excoffier. 2000. Arlequin: A software for population genetics data analysis. Version 2. Genetics and Biometry Lab, Dept of Anthropology, University of Geneva, Switzerland. http://anthro.unige.ch/software/arlequin/
Schwede, T., J. Kopp, N. Guex, and M. C. Peitsch. 2003. SWISS-MODEL: an automated protein homology-modeling server. Nucleic Acids Res. 31: 3381-3385.
Segelbacher, G., D. Kabisch, M. Stauss, and J. Tomiuk. 2005. Extra-pair young despite strong pair bonds in the European nuthatch (*Sitta europaea*). J. Ornithol. 146:99-102.
Shapiro, L. H., and J. P. Dumbacher. 2001. Adenylate Kinase Intron 5: a new nuclear locus for avian systematics. Auk 118:248-255.
Slatkin, M. 1987. Gene flow and the geographic structure of natural populations. Science 236:787-792.

Sorenson, M. D., J. C. Ast, D. E. Dimcheff, T. Yuri, D. P. Mindell. 1999. Primers for a PCR-based approach to mitochondrial genome sequencing in birds and other vertebrate. Mol. Phylogenet. Evol. 12:105-112.
Sousa-Santos, C., J. I. Robalo, M.-J. Collarrs-Pereira, and V. C. Almada. 2005. Heterozygous indels as useful tools in the reconstruction of DNA sequences and in the assessment of ploidy level and genomic constitution of hybrid organisms. DNA Sequence 16:462-467.
Spellman, G. M., and J. Klicka. 2006. Testing hypotheses of Pleistocene population history using coalescent simulations: phylogeography of the pygmy nuthatch (*Sitta pygmaea*). P. Roy. Soc. B. 273:3057-3063.
Stamatakis, A., P. Hoover, and J. Rougemont. 2008. A rapid bootstrap algorithm for the RAxML web servers. Syst. Biol. 57:758-771.
Stepanyan, L. S. 2003. Conspectus of the ornithological fauna of Russia and adjacent territories (within the borders of the USSR as a historic region). Academkniga, Moscow, Russia.
Stephens, M., N. Smith, and P. Donnelly. 2001. A new statistical method for haplotype reconstruction from population data. Am. J. Hum. Genet. 68:978-989.
Stephens, M., and P. Scheet. 2005. Accounting for decay of linkage disequilibrium in haplotype inference and missing-data imputation. Am. J. Hum. Genet. 76:449-462.
Stjernberg, T., 1979. Breeding biology and population dynamics of the scarlet rosefinch *Carpodacus erythrinus*. Acta Zool. Fennica 157:1-88.
Strasburg, J. L., and L. H. Reiseberg. 2010. How robust are "isolation with migration" analyses to violations of the IM model? A simulation study. Mol. Biol. Evol. 27:297-310.
Svendsen, J. I., H. Alexanderson, and V. I. Astakhov et al. 2004. Late Quaternary ice sheet history of north Eurasia. Quaternary Sci. Rev. 23:1229-1271.
S□tre, G.-P., T. Borge, J. Lindell, T. Moum, C. R. Primmer, B. C. Sheldon, J. Haavie, A. Johnsen, and H. Ellegren. 2001. Speciation, introgressive hybridization and nonlinear rate of molecular evolution in flycatchers. Mol. Ecol. 10:737-749.
Tamura, K., J. Dudley, M. Nei, and S. Kumar. 2007. MEGA4: molecular Evolutionary genetics Analysis (MEGA) software version 4.0. Mol. Biol. Evol. 24:1596-1599.
Tavares, E. S., G. H. de Kroon, and A. Baker. 2010. Phylogenetic and coalescent analysis of three loci suggest that the water rail is divisible into two species, *Rallus aquaticus* and *R. indicus*. BMC Evol. Biol. 10:226.
Tieleman, B. I., M. A. Versteegh, A. Fries, B. Helm, N. J. Dingemanse, H. L. Gibbs, and J. B. Williams. 2009. Genetic modulation of energy metabolism in birds through mitochondrial function. Proc. R. Soc. B 276:1685-1693.
Tourasse, N. J., and W.-H. Li. 2000. Selective constraints, amino acid composition, and the rate of protein evolution. Mol. Biol. Evol. 17:656-664.
Tusnády, G.E., and I. Simon. 2001. The HMMTOP transmembrane topology prediction server. Bioinformatics 17:849-850. http://www.enzim.hu/hmmtop.
Tyrberg, T. 1998. Pleistocene birds of the Palearctic: a catalogue, Vol. 27. Nuttall Ornithological Club, Cambridge, MA.
Weir, J.T., Schluter, D., 2008. Calibrating the avian molecular clock. Mol. Ecol. 17, 2321-2328.

Walstrom, V. W., J. Klicka, and G. M. Spellman. 2012. Speciation in the White-breasted Nuthatch (*Sitta carolinensis*): a multilocus perspective. Mol. Ecol. 21:907-920.
Wares, J. P. 2010. Natural distributions of mitochondrial sequence diversity support new null hypotheses. Evolution 64:1136-1142.
Warren, D. L., R. E. Glor, and M. Turelli. 2008. Environmental niche equivalency versus conservatism: quantitative approaches to niche evolution. Evolution 62:2868-2883.
Warren, D. L., R. E. Glor, and M. Turelli. 2010. ENMTools: a toolbox for comparative studies of environmental niche models. Ecography 33:607-611.
Weir, J. T., and D. Schluter. 2008. Calibrating the avian molecular clock. Mol. Ecol. 17:2321-2328.
Wise, C. A., M. Sraml, and S. Easteal. 1998. Departure from neutrality at the mitochondrial NADH dehydrogenase subunit 2 gene in humans, but not in chimpanzees. Genetics 148:409-421.
Wu, Y. 2012. Coalescent-based species tree inference from gene tree topologies under incomplete lineage sorting by maximum likelihood. Evolution 66:763-775.
Yang, Z. 1997. PAML: a program package for phylogenetic analysis by maximum likelihood. Comput. Appl. Biosci. 13:555-556.
Yang, Z. 2007. PAML 4: a program package for phylogenetic analysis by maximum likelihood. Mol. Biol. Evol. 24:1586-1591.
Yang, Z, and J. P. Bielawski. 2000. Statistical methods for detecting molecular adaptation. Trends Ecol. Evol. 15:496-503.
Yang, Z., W. J. Swanson, and V. D. Vacquier. 2000. Maximum-likelihood analysis of molecular adaptation in abalone sperm lysine reveals variable selective pressures among lineages and sites. Mol. Biol. Evol. 17: 1446-1455.
Yuri, T., R. W. Jernigan, R. T. Brumfield, N. K. Bhagabati, and M. J. Braun. 2009. The effect of marker choice on estimated levels of introgression across an avian (Pipridae: *Manacus*) hybrid zone. Mol. Ecol. 18:4888-4903.
Zink, R. M. 2005. Natural selection on mitochondrial DNA in *Parus* and its relevance for phylogeographic studies. P. Roy. Soc. B. 272:71-78.
Zink, R. M., S. V. Drovetski, and S. Rohwer. 2006. Selective neutrality of mitochondrial ND2 sequences, phylogeography and species limits in *Sitta europaea*. Mol. Phyl. Evol. 40:679-686.
Zink, R. M., and G. F. Barrowclough. 2008. Mitochondrial DNA under siege in avian phylogeography. Mol. Ecol. 17:2107-2121.
Zink, R. M., A. Pavlova, S. Drovetski, and S. Rohwer. 2008. Mitochondrial phylogeographies of five widespread Eurasian bird species. J. Ornithol. 149:399-413.